EUROPEAN JOINT PROGRAMME
FOR THE INTEGRATION OF
RADIATION PROTECTION RESEARCH
CONCERT

LEU TRACK

EJP-CONCERT

European Joint Programme for the Integration of Radiation Protection Research

H2020 – 662287

D9.99 - Final report of the LEU_TRACK project

Lead Author: HMGU, NNK, PHE, GUF

(Katalin Lumniczky, Soile Tapio, Christophe Badie, Franz Rödel)

Reviewer(s): Géza Sáfrány

Work package / Task	WP 9; ST9.5 (LEU-TRACK)	SST 4.1, 4.2, 4.3
Deliverable nature:	**Report**	
Dissemination level: (Confidentiality)	**Public**	
Contractual delivery date:	**M56 (Jan 2020)**	
Actual delivery date:	**Postponed to M58 (March 2020)**	
Version:	**1**	
Total number of pages:	**34**	
Keywords:	**Extracellular vesicles (EVs), bone marrow-derived EVs in radiation leukaemogenesis, blood-derived EVs**	
Approved by the coordinator:	**07/04/2020 (M59)**	
Submitted to EC by the coordinator:	**07/04/2020 (M59)**	

Abstract

Radiation-induced leukaemia develops as a result of direct radiation damage to stem cells and an altered intercellular communication between the stem cell pool and its microenvironment. Bystander signalling, meaning detection of radiation damage in cells not directly hit by radiation, is particularly important in the manifestation of low dose radiation effects in the bone marrow and thus it is reasonable to assume that it plays a role in low dose-induced leukaemogenesis as well. Extracellular vesicles (EVs) due to their complex protein and RNA content are major mediators of bystander signals. The main objective of LEU-TRACK was to study the role of bone marrow-derived EVs in radiation leukaemogenesis in a murine model genetically prone to develop leukaemia after irradiation. We also aimed to investigate major molecular and cellular mechanisms mediated by EVs. In the first part of the project mice were either irradiated or injected with EVs isolated from the bone marrow of irradiated animals and the incidence as well as time of onset of leukaemia was followed. In parallel, the miRNA and protein content of bone marrow-derived EVs were analysed by omics approaches. The surface markers of isolated EVs were analysed by flow cytometry in order to identify major cellular populations, which secrete them and to determine radiation-induced differences in this process. Finally, a small clinical study was initiated within LEU-TRACK, where the miRNA and protein content of blood-derived EVs from radiotherapy-treated leukaemia were analysed. Our main results indicated that EVs from irradiated mice contributed to the development of various haematological abnormalities and most probably had an impact on the incidence of radiation-induced leukaemogenesis. We also showed comparable quantitative and functional alterations in the bone marrow cells of EV-treated mice compared to directly irradiated mice. There was a strong overlap in the type of miRNAs and proteins as well as regulated molecular and cellular pathways in the EVs from low and high dose irradiated mice and, in some cases, quantitative changes were dose-dependent. Blood-derived EVs from leukaemia patients were suitable candidates to identify disease and radiation-related biomarkers. In summary, our work contributed to a better understanding of low dose irradiation induced bystander responses in the bone marrow and leukaemia development and we provided new knowledge on the role of EVs within this process.

Table of Content

Introduction and objectives

Recently published epidemiological studies clearly show an elevated risk of leukaemia in radiation workers exposed to protracted low dose radiation exposure (Gillies et al, 2019; Schubauer-Berigan et al, 2015). Basic mechanisms leading to low dose IR-induced leukemogenesis and evaluation of health risks attributable to low dose exposures represent key gaps in radiation protection research. While IR-induced direct damage to the haematopoietic stem cell pool is suggested to be a major driver in disease development after higher doses, IR-induced leukaemia at low doses most probably involves additional mechanisms distinct from those at high doses. EVs are major vehicles of intercellular communication due to their complex cargo. The LEU-TRACK project proposed to study mechanisms and pathways how BM-derived EVs, by influencing the communication between the different cellular components can induce BM damage and thus modulate low dose IR-induced leukaemia.

The initial major objectives of LEU-TRACK were the following:

➢ To study how EVs originating from irradiated animals can influence leukaemogenesis in genetically susceptible mice.
➢ To investigate the mechanism of radiation-induced leukaemogenesis by studying the role of bone marrow-derived EVs from irradiated animals in the crosstalk between the bone marrow microenvironment and the stem cell compartment, by investigating the EV cargo and by quantifying cellular and molecular changes in the EV-target cells and tissues.
➢ To identify EV-mediated markers of radiation exposure and leukaemia in the blood of irradiated mice and to compare these markers with EV-derived markers identified in blood samples from leukaemia patients treated with total body irradiation.

Scientific approaches and achieved results:

I. Follow up of leukaemia incidence in irradiated and/or EV-treated mice

At NNK 10-12 week-old male CBA/H mice were total body irradiated (TBI) with 0 Gy (control), 0.1 Gy and 3 Gy X-rays. BM was isolated from treated animals, BM cells were pelleted and BM-derived EVs were isolated from the BM supernatant with Exoquick precipitation solution (System Biosciences). EVs from all the samples were characterized by Western blotting (WB), dynamic light scattering (DLS) and flow cytometry (FC). DLS measurements showed that isolated nanoparticles had an average diameter of 250 nm, varying between 80 and 600 nm, indicating that both small, exosome-like particles and larger, microvesicle-like particles were present in the isolates. WB analysis indicated that EVs carried EV-specific markers, such as different tetraspanins (CD9, CD63 and CD81) and TSG101 while lacking calnexin (endoplasmic reticulum marker indicating cellular protein contamination). EV markers were validated by FC as well. Plasma EVs were isolated similarly.

BM-derived EVs were injected intravenously into naïve or pre-irradiated mice for long-term follow-up in order to monitor the influence of EVs on leukemogenesis. A total of 761 mice of different experimental groups (**Table 1**) are being followed either until they become terminally ill or reach the age of 24 months, when mice are euthanized and investigated for signs of leukaemia or other diseases.

Treatment group	Treatment	Number of mice

I/1	0 Gy (sham-irradiated, control)	51
I/2	0.1 Gy	90
I/3	3 Gy	51
II/4	0 Gy EV (naïve mice injected with BM-derived EVs from sham-irradiated mice)	51
II/5	0.1 Gy EV (naïve mice injected with BM-derived EVs from 0.1 Gy mice)	89
II/6	3 Gy EV (naïve mice injected with BM-derived EVs from 3 Gy mice)	49
III/7	0 Gy + 0 Gy EV (sham irradiated mice injected at the same age as groups III/9-12 with EVs from sham-irradiated mice)	51
III/8	0 Gy + 3 Gy EV (sham irradiated mice injected at the same age as groups III/9-12 with EVs from 3 Gy mice)	49
III/9	0.1 Gy + 0 Gy EV (0.1 Gy irradiated mice injected with EVs from sham irradiated mice)	90
III/10	0.1 Gy + 3 Gy EV (0.1 Gy irradiated mice injected with EVs from 3 Gy mice)	90
III/11	3 Gy + 0 Gy EV (3 Gy irradiated mice injected with EVs from sham-irradiated mice)	50
III/12	3 Gy + 3 Gy EV (3 Gy irradiated mice injected with EVs from 3 Gy mice)	50

Table 1: *Treatment groups and number of animals in each group*

Criteria of leukaemia diagnosis: a) deterioration of general health condition (body weight loss, reduced motility, loss of appetite, abnormal body hair, pale soles), enlarged abdomen with palpable liver and/or spleen; b) histopathological analysis performed by an animal pathologist; c) phenotypical image of BM cells by FC (e.g. leucocytosis, increased myeloid progenitors, loss of common myeloid-monocytic markers, increased haematopoietic stem cells and leukaemic stem cells); d) loss of SFPI1 allele (investigated by FISH at NNK) and detection of acute myeloid leukaemia (AML)-specific point mutation in the gene (performed by pyrosequencing at PHE).

At the time of this report, approx. 62% of the mice have been euthanized either because they were ill or reached the age of 24 months and are being investigated for leukaemia diagnosis. Figure 1 shows the number of already confirmed cases of leukaemia. So far, 7.8% of mice treated with 3 Gy TBI, 13.2% of mice treated with 3 Gy+3 Gy EV and 12% of mice treated with 3 Gy+0 Gy EV have developed AML. Until now, 1 mouse irradiated with 0.1 Gy had AML (1.1%) and no AML case was detected in solely EV treated or control mice (***Figure 1***). Nevertheless, other haematological malignancies are suspected based on the BM phenotype (such as acute lymphoblastic leukaemia), which need to be confirmed by histology.
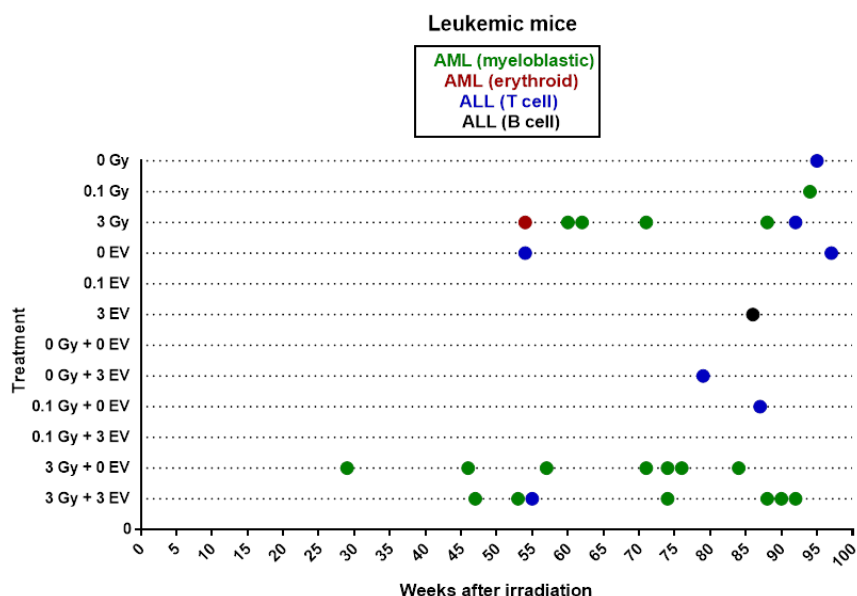
Figure 1. *Development of AML in CBA mice treated with IR and/or EV injection. Dots represent individual cases of leukaemia.*

A panel of other malignancies also increased. Liver tumors are by far the most common tumors. Apart of malignant liver tumors, a panel of other liver alterations (benign tumors, diffuse hepatomegaly with extramedullar haematopoiesis) is also being detected. At present it seems that the frequency of liver alterations increases in the aging mouse. We also detected an increased frequency of harderian gland tumors of the eye as well as lung tumors. While eye tumors developed only in the irradiated mice, liver and lung tumors developed in control animals as well.

II. Analysis of EV phenotype and cargo

Part of the isolated BM-derived EVs were used for phenotypical (NNK), proteomic (HMGU) and miRNA (PHE) analysis. EVs were isolated from BM tissue and plasma in vivo using Exoquick-TC solution for phenotyping and for miRNA profiling and by ultracentrifugation for proteomic analysis. DLS measurements indicated that the average diameter of the EVs was 228 nm (±52 nm).

A. Analysis of EV phenotype

EV phenotype was investigated by flow cytometry using a dedicated flow cytometer suitable for visualisation of vesicles above 100 nm.

Within the EV gates defined on size and light scattering properties EVs were further identified using the CD9, CD63 and CD81 EV-specific surface markers. While distribution of these markers on the different EV subpopulations might vary, presence of any of them is an obligate criterion for EV identification.

Most BM-derived EVs from control mice expressed integrins (30.5% and 42.1% of EVs were CD29+ and CD44+, respectively) typical for MSCs but present on other BM subpopulations as well (*Table 2* and *Figure 2*). Since the fraction of MSCs represents less than 1.5% of the Lin-BM cells, this indicates that most probably EVs

harbouring integrin markers are released by different cell types, not only MSCs and represents an abundant EV fraction in the BM. EVs carrying CD11b or Gr1 markers can be attributed to granulocyte-myeloid progenitors (GMP), though these markers are also present on other, more differentiated cells of myeloid origin. While the fraction of GMPs in the BM of control mice was 22%, the fraction of EVs harbouring GMP markers were between 3.1% and 4% (**Table 2**). Ter119+ cells are of erythroid origin consisting of erythroid progenitors and more differentiated erythroid cells. Their fraction in the BM was altogether 60.3%. Though, EVs carrying the Ter119 marker represented only 0.227% of total BM-derived EVs (**Table 2**). The presence of CD90.2 is rather specific to lymphoid progenitors (LPs), so EVs carrying CD90.2 can be attributed to LPs. Similarly, CD41 is also specific for megakaryocytes, thus EVs carrying this marker are considered of megakaryocyte origin. The fraction of LP- and megakaryocyte-derived EVs was 4.2 and 5.5% respectively (**Table 2**), while the fraction of LP cells and megakaryocytes in the BM was 1.6 and 1.4% respectively. These data indicate that EV production by LPs and megakaryocytes were more abundant than EV production by myeloid or erythroid cells.

	CD29	CD44	cKit	CD90.2	Ter119	CD11b	Gr-1	CD41	CD61
0 Gy	30.5 (±5.64)	42.07 (±18.2)	0.832 (±0.41)	4.294 (±2.71)	0.227 (±0.17)	3.157 (±1.05)	4.057 (±1.262)	5.537 (±2.74)	0.087 (±0.036)
0.1 Gy	34.46 (±9.4)	47.06 (±14.2)	0.653 (±0.34)	11.25 (±1.14)*	0.328 (±0.17)	3.19 (±1.39)	6.347 (±1.36)	11.44 (±5.25)	0.103 (±0.012)
3 Gy	13.86 (±4.05)***	24.71 (±9.75)*	3.478 (±1.52)	9.146 (±4.44)	1.345 (±0.44)*	3.748 (±0.49)	8.18 (±4.31)	9 (±3.89)	0.365 (±0.11)

Table 2. *The effect of ionizing radiation on the percentage of EVs with typical bone marrow cell markers. Mice were irradiated with the indicated doses and 24 hours after irradiation EVs were isolated from bone marrow supernatant and labelled with EV-specific markers followed by antibodies against typical bone marrow cell markers and analysed by flow cytometry as described in the Materials and methods. Data represent mean (±SD) percentages of EVs within the HOB gate. Four mice were pooled for one sample and min. 4 parallels were used for statistical analysis. Statistical significance was calculated with Students's t-test, changes are significant if *p<0.05, **p<0.01, ***p<0.001 compared to 0 Gy controls.*

Ionizing radiation did not influence EV size. Low dose ionizing radiation did not change significantly the fraction of the different types of EVs in the BM with the exception of EVs harbouring lymphoid progenitor (LP) markers, which increased significantly (**Table 2**). High dose (3 Gy) irradiation induced a significant decrease in EVs carrying the CD29 or CD44 integrin markers. Other EVs either did not change or increased after irradiation with 3 Gy. The most pronounced increase in EV production after 3 Gy was noted in HSC-related EVs carrying the c-kit marker. While the HSC pool decreased 18-fold after irradiation with 3 Gy, EV secretion increased with 4.2 fold. Strong increase was seen also in EV secretion by myeloid cells (carrying the CD11b or Gr1 marker) and LPs (carrying the CD90.2 marker) after 3 Gy, albeit changes were milder than in HSC-derived EV secretion (**Figure 3**).

In conclusion, EVs carry markers characteristic for the different BM subpopulations but the presence of these markers allows identification of the cellular origin of the EVs only to a limited extent. Low-dose irradiation had very limited effect on EV secretion. High dose ionizing radiation induced a strong rearrangement in the pool of BM-derived EVs which were markedly different from BM cell pool rearrangements. This indicates that ionizing radiation effects on the EV secretion by the different BM cell subpopulations were cell type-specific and did not correlate with the radiosensitivity of the particular cell subpopulation.
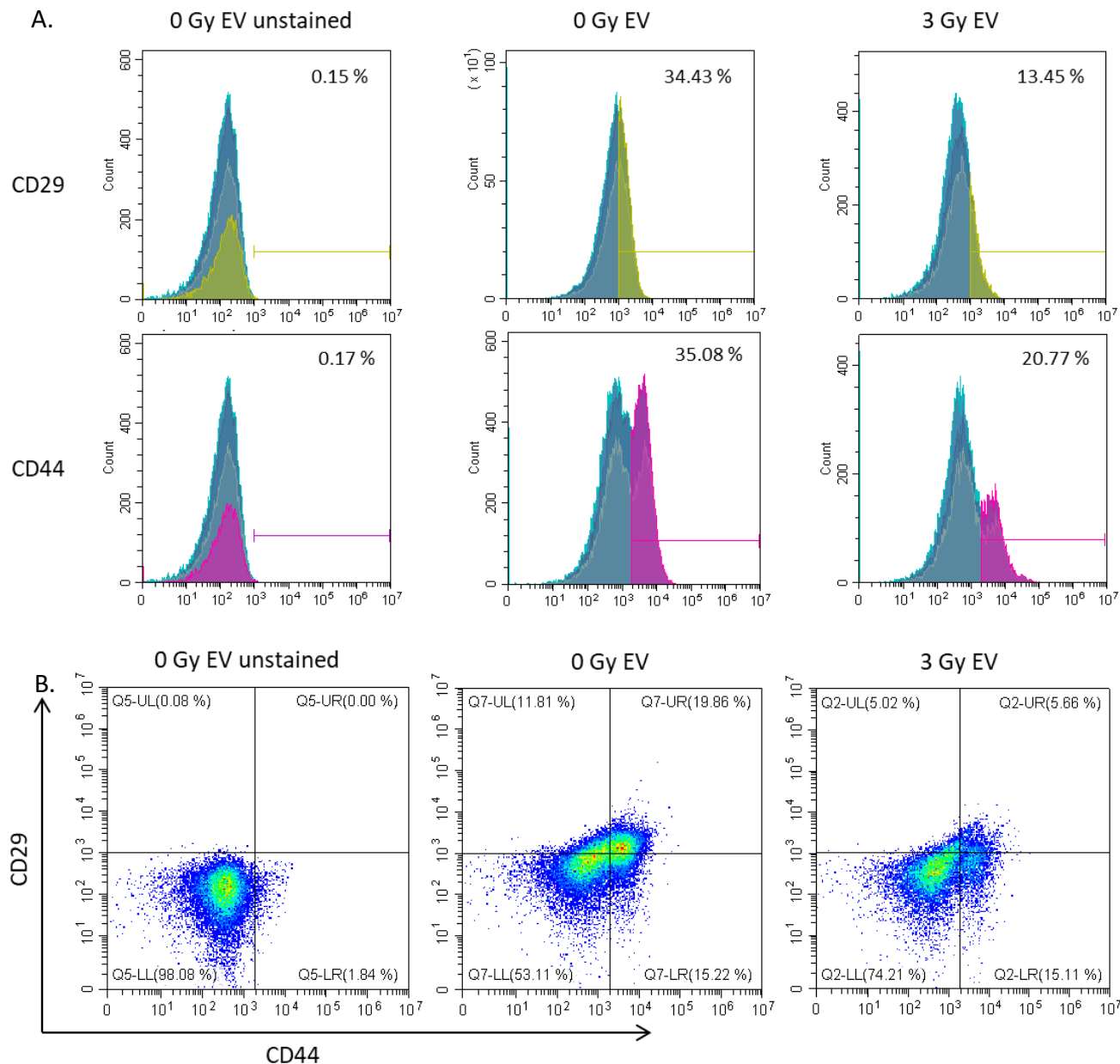
Figure 2. *Representative figure of EVs with CD29 and CD44 markers: histograms (A) and dot plots (B). EVs were isolated from the bone marrow of mice irradiated with the indicated doses. EVs were labelled with antibodies against typical markers of bone marrow cell populations (here: CD29 and CD44) as described in the Materials and methods section. Analysis is performed on EVs gated based on their EV-marker (CD9/CD63/CD81) positivity.*
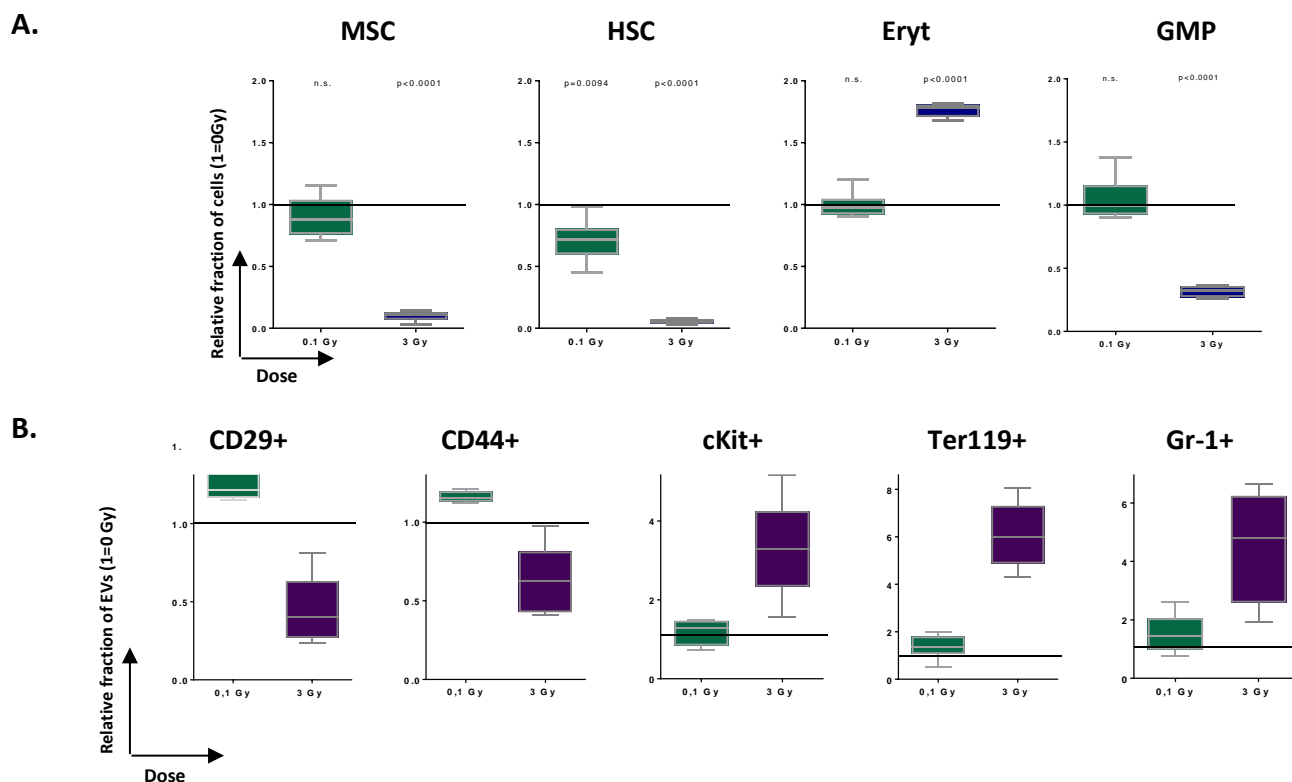
A.

B.

Figure 3. *Relative changes in the fraction of bone marrow cell subpopulations (A) and EVs (B) in irradiated mice compared to controls. Mice were irradiated with the indicated doses and 24 hours after irradiation bone marrow cells and EVs were isolated, labelled and analysed by flow cytometry as described in the Materials and methods. Cell types (A) and EV types (B) are shown above the individual graphs. Error bars represent SD, p values are shown above the graphs.*

B. Analysis of EV miRNA content

MiRNA profile of bone marrow-derived EVs from directly irradiated animals (0.1 Gy and 3 Gy)

The total RNA extracted from the bone marrow derived EVs from the 0 Gy, 0.1 Gy and 3 Gy groups was run in a nCounter panel which includes probes to identify 800 different murine miRNAs. The 0.1 Gy dose presented 4 significant upregulated miRNAs (***Table 3***) with fold changes ranging from 8 to 13-fold with p-values below 0.05. Pathway analysis of the top ten most significant up- and downregulated miRNAs from the 0.1 Gy dose (***Table 4***) showed that the most relevant miRNAs regulated by the low dose target genes are involved in endocytosis, cell cycle, MAPK signaling, ubiquitin-mediated proteolysis, leukocyte transendothelial migration, regulation of actin cytoskeleton and adherent junction.

The 3 Gy dose showed a more extensive list of miRNAs regulated than at 0.1 Gy (***Table 5***). From the 20 miRNAs significantly regulated, only 2 were downregulated (mmu-miR-709 and mmu-miR 706). When comparing both doses, four different miRNAs were found to be statistically relevant in 0.1 Gy and 3 Gy: mmu-miR-761, mmu-miR-129-5p, mmu-miR-669g, and mmu-miR-34b-5p (***Table 6***). Therefore the 0.1 Gy response seems to be conserved in 3 Gy. All miRNAs have a higher fold change at 3Gy when compared to 0.1Gy, suggesting a dose-dependent upregulation, rather than an on/off mechanism of upregulation. Pathway analyses of the 3 Gy group (***Table 7***) showed an extension of the pathways identified at 0.1 Gy.

Name	Group1	Group2	Fold Change	P-value	FDR
mmu-miR-761	2.00	13.00	4.67	0.03	1.00
mmu-miR-129-5p	3.00	18.00	4.75	0.04	1.00
mmu-miR-669g	2.00	10.00	3.67	0.05	1.00
mmu-miR-34b-5p	1.00	8.00	4.50	0.05	1.00

Table 3: *Control vs 0.1 Gy significant miRNAs. Analysis performed with DIANA-miRPath v.3.0 software. Group1, control; Group2, 0.1 Gy; FDR, false discovery rate.*

Upregulated miRNAs	Downregulated miRNAs
Endocytosis	Adherens junction
Cell cycle	Leukocyte transendothelial migration
MAPK signalling	Regulation of actin cytoskeleton
Ubiquitin-mediated proteolysis	

Table 4: *Control vs 0.1Gy differentially regulated cellular pathways.*

Name	Group1	Group2	Fold Change	P-value	FDR
mmu-miR-709	170.00	11.00	0.07	3.3e-4	0.08
mmu-miR-34b-5p	2.00	33.00	11.33	2.4e-3	0.20
mmu-miR-323-5p	2.00	40.00	13.67	2.6e-3	0.20
mmu-miR-761	3.00	34.00	8.75	4.9e-3	0.23
mmu-miR-291a-3p	3.00	32.00	8.25	5.3e-3	0.23
mmu-miR-323-3p	2.00	25.00	8.67	6.8e-3	0.23
mmu-miR-1946a	2.00	28.00	9.67	6.9e-3	0.23
mmu-miR-1933-5p	11.00	90.00	7.58	9.9e-3	0.29
mmu-miR-1898	3.00	30.00	7.75	0.01	0.29
mmu-miR-669g	3.00	26.00	6.75	0.01	0.29
mmu-miR-695	5.00	51.00	8.67	0.01	0.29
mmu-miR-706	32.00	4.00	0.15	0.02	0.30
mmu-miR-669h-5p	15.00	98.00	6.19	0.02	0.38
mmu-miR-338-5p	12.00	61.00	4.77	0.03	0.54
mmu-miR-466k	2.00	19.00	6.67	0.04	0.54
mmu-miR-1942	17.00	84.00	4.72	0.04	0.58
mmu-miR-129-5p	4.00	32.00	6.60	0.04	0.58
mmu-miR-688	6.00	33.00	4.86	0.05	0.60
mmu-miR-878-5p	8.00	44.00	5.00	0.05	0.60
mmu-miR-1904	6.00	42.00	6.14	0.05	0.60

Table 5. *Control vs 3 Gy significantly differentially expressed miRNA. Analysis performed with DIANA-miRPath v.3.0 software. Group1, control; Group2, 3 Gy; FDR, false discovery rate.*

miRNA	Fold change at 0.1Gy	Fold change at 3Gy
mmu-miR-761	4.67	8.75
mmu-miR-129-5p	4.75	6.60
mmu-miR-669g	3.67	6.75
mmu-miR-34b-5p	4.50	11.33

Table 6. Comparison of the miRNA profiles between 0.1 Gy and 3 Gy.

Upregulated miRNAs	Downregulated miRNAs	
Endocytosis	Adherens junction	Pathways in cancer
Cell cycle	Leukocyte transendothelial migration	mTOR signalling pathway
MAPK signalling	Regulation of actin cytoskeleton	Acute myeloid leukaemia
Ubiquitin-mediated proteolysis	Fatty acid biosynthesis	Wnt signalling pathway
Regulation of actin cytoskeleton	Proteoglycans in cancer	Transcriptional misregulation in cancer
Phosphatidylinositol signalling system	Lysine degradation	FoxO signalling pathway
D-glutamine and D-glutamate metabolism	N-Glycan biosynthesis	
Inositol phosphate metabolism	Protein processing in ER	
T cell receptor signalling pathway	Hippo signalling pathway	

Table 7. Control vs 3 Gy differentially regulated cellular pathways.

Clustering analysis performed with BRB array1 tools showed clear up- and downregulated clusters of miRNAs which include the miRNAs identified using Diana tools software. These results demonstrate that the miRNA cargo of the EVs is modulated by irradiation and their response is not random. Besides, dose correlation analysis identified 13 miRNAs which show a strong dose-response (**Table 8**) with correlation coefficients between 0.95 and 0.84.

Genes significantly correlated with Quantitative Trait:

Table - Sorted by p-value of the univariate test
The first 13 genes are significant at the nominal 0.001 level of the univariate test

	Correlation coefficient	Parametric p-value	FDR	UniqueID
1	0.953	< 1e-07	< 1e-07	mmu-miR-323-5p
2	0.888	9.17e-05	0.00592	mmu-miR-1933-5p
3	0.888	9.17e-05	0.00592	mmu-miR-1961
4	0.888	9.17e-05	0.00592	mmu-miR-338-5p
5	0.888	9.17e-05	0.00592	mmu-miR-504
6	0.884	0.0001922	0.0103	mcmv-miR-m107-1-5p
7	0.875	0.0003089	0.0125	mmu-miR-290-5p
8	0.874	0.0003089	0.0125	mmu-miR-708
9	0.857	0.0005971	0.0161	mmu-miR-181c
10	-0.857	0.0005971	0.0161	mmu-miR-2146
11	0.859	0.0005971	0.0161	mmu-miR-467h+mmu-miR-669d+mmu-miR-669l
12	0.857	0.0005971	0.0161	mmu-miR-669j
13	-0.843	0.0009695	0.0222	mmu-miR-93

Table 8. miRNAs correlated with the dose. BRB array tools correlation analyses showed 11 miRNAs positively and 2 negatively correlated with dose.

MiRNA profile of plasma-derived EVs from directly irradiated animals

The miRNA profiling in plasma EVs was more challenging than in bone marrow EVs due to the miRNA concentrations obtained. Therefore, to be able to obtain miRNA information, we decided to perform next- generation Sequencing (NGS) instead of nCounter analyses. The sequencing analyses were outsourced to Arraystar (USA). NGS was performed in an Illumina NextSeq 500 system and miRDeep2 software was used to quantify known miRNA and differentially expressed miRNA were filtered using R package edgeR.

Differentially expressed analysis showed two miRNAs to be the highest upregulated miRNAs at both doses, mmu-miR-378a-5p and 378b. Pathway analysis for miR-378b targets identified acute myeloid leukemia pathway together with insulin and mTOR signaling pathways which are involved in cell metabolism, differentiation and survival. Pathway analysis including all the differentially upregulated miRNAs showed pathways involved in several cancers together with metabolism, cell growth, proliferation, survival signaling pathways (PI3K/AKT pathway, mTOR, cAMP, Rap1, Ras) which are dysregulated in several types of cancer (***Figure 4***).

Figure 4. *Top 10 significant pathways of the gene targets of the upregulated miRNAs. Ordered from top to bottom by P-value, with the most significant pathway on the top. The P-values calculated by Fisher's exact test are used to estimate the statistical significance of the enrichment of the pathways between the two group.*

The top ten differentially expressed downregulated miRNAs showed that common downregulated miRNAs are also present in both doses. Pathway analysis predicted pathways which might be potentiated due to the decrease of miRNAs targeting the genes involved in them (***Figure 5***). Within these pathways, there was MAPK, endocytosis, some cancers, cGMP-PKG and glycerophospholipids pathways amongst others.

Down regulated miRNA
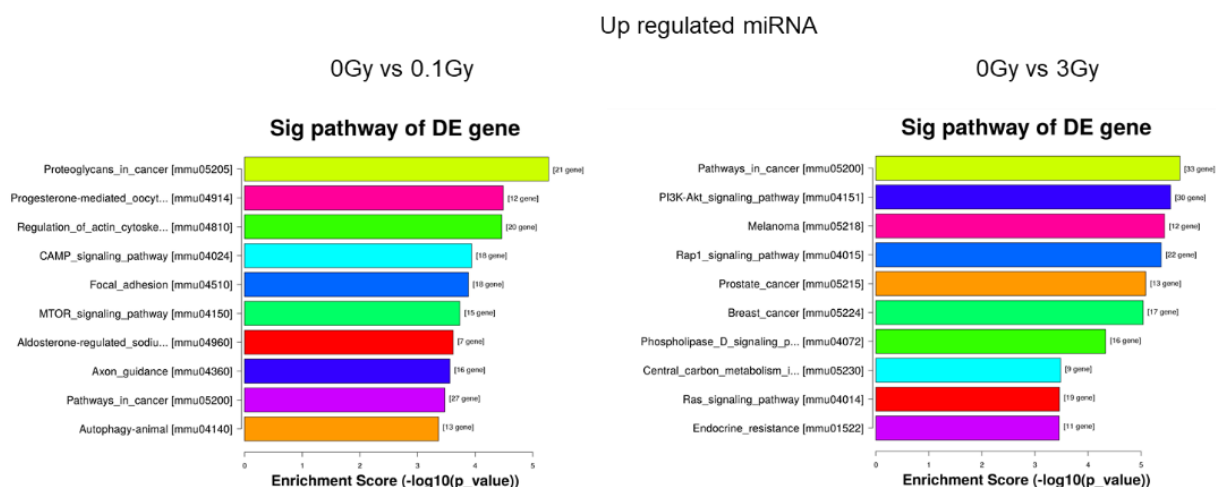
0Gy vs 0.1Gy

0Gy vs 3Gy
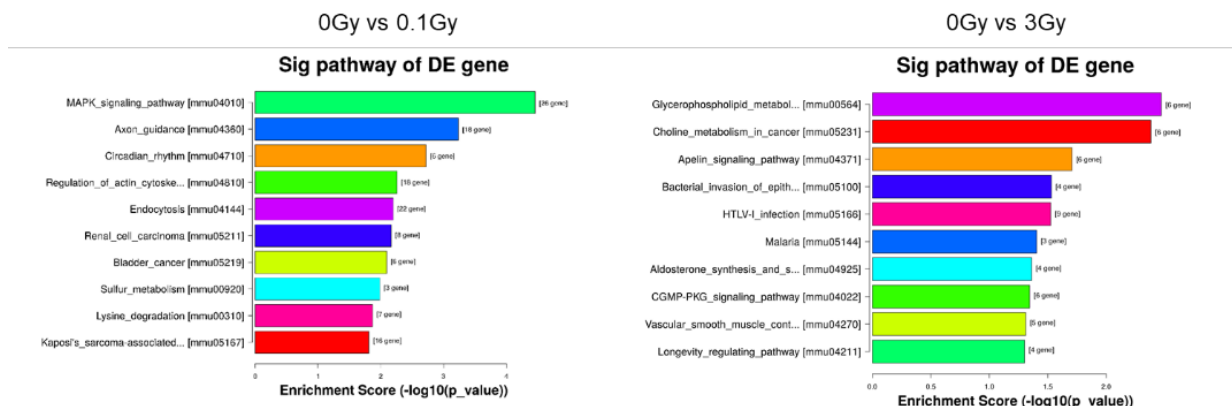
Figure 5. *Top 10 significant pathways of the gene targets of the downregulated miRNAs***.** *Ordered from top to bottom by P-value, with the most significant pathway on the top. The P-values calculated by Fisher's exact test are used to estimate the statistical significance of the enrichment of the pathways between the two group.*

Gene ontology analysis demonstrated that the genes that the miRNAs targeted in both doses are involved in similar biological processes with similar functions. Hierarchy clustering analyses were performed taking together all the miRNA identified by sequencing. The analyses presented dose-dependent upregulated and downregulated clusters of miRNAs.

In conclusion, our data show that miRNA response does not operate in a binary fashion, either upregulated or downregulated by ionizing radiation; it instead appears to be correlated to dose. As dose increases, more pathways are involved via IR-induced modifications to miRNA expression. The results suggest that IR induces similar miRNA expression patterns at low and high doses (only differences at the level of regulation-lower fold changes at lower dose) and their level of expression is dose-dependent for some of them. Therefore, the miRNAs dose response at 0.1 Gy is not qualitatively different to 3Gy, as much as it is more limited in bone marrow EVs as well as plasma EVs. The dose response at 3 Gy expands upon an initial limited response at 0.1 Gy; it is likely the pathways upregulated at 0.1 Gy are triggered at a lower dose response than those only activated at 3 Gy. Clustering analysis identified clusters of miRNAs which showed a strong dose-dependency, therefore miRNA response is not random. Pathway analysis indicate cell differentiation, growth, proliferation and metabolism related pathways to be the common miRNAs targets for both doses. Dysregulation of these pathways are common in several cancers.

C. Analysis of EV protein content

In the serum-derived EVs, 310 proteins were identified in total. In the bone marrow-derived EVs, 2103 proteins were identified in total. In the serum- and bone marrow-derived EVs, 243 proteins and 1772 proteins were identified with at least two unique peptides, respectively.

No clustering was observed in principal component analysis (PCA) based on the protein abundances in serum-derived EVs. In contrast, the proteome features representing bone marrow-derived EVs from 0 Gy and 3 Gy treated mice showed clustering with the dose (***Figure 6***).
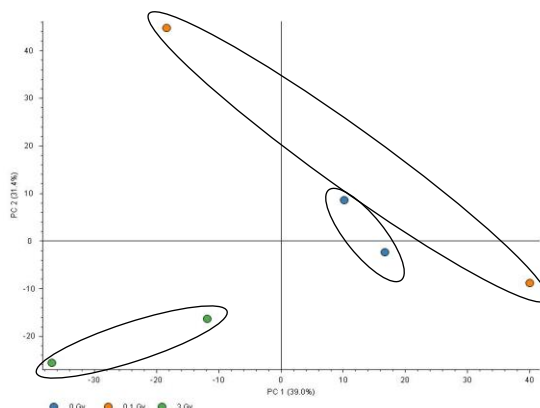
Figure 6. *Principal component analysis (PCA) of bone marrow EVs from sham-irradiated mice (0 Gy) and irradiated mice (0.1 Gy and 3 Gy) based on protein abundances. Biological replicates for each dose are grouped and indicated by ellipses.*

In the serum-derived EVs from mice treated with 0.1 Gy, 91 proteins were deregulated (57 downregulated, 34 upregulated) using a fold change cut-off of +1.3. With a similar cut-off, 106 proteins were deregulated (62 downregulated and 44 upregulated) after 3 Gy treatment. There was no significant dose-dependent increase in the number of deregulated proteins. Amongst the deregulated proteins, 63 proteins were common at both radiation doses. This represents 47% of all deregulated proteins. Only in two cases the direction of deregulation was opposite at these two doses. The 63 common deregulated proteins were subjected to an in silico enrichment analysis (***Figure 7***) with the STRING web tool (https://string-db.org/). One major cluster and two minor clusters were observed, the major one representing mainly proteins belonging to defense or stress responses or responses to a stimulus.

Figure 7. *(A) A Venn diagram showing the number of deregulated proteins in serum-derived EVs from mice treated with 0.1 Gy or 3 Gy TBI. (B) STRING enrichment analysis of the 63 common deregulated proteins is shown. Proteins, belonging to defence response (GO:0006952, FDR 1.12 × 10-16, green), response to stress (GO:0006950, FDR 1.12 × 10-6, blue), and response to stimulus (GO:0050896, FDR 8.79 × 10-6, red), are marked.*

In the bone marrow derived EVs from the mice treated with 0.1 Gy, altogether 148 proteins were deregulated of which 5 were downregulated and 143 upregulated. After the 3 Gy treatment, 152 proteins were deregulated (68 downregulated and 84 upregulated). Similar to serum-derived EVs, the number of deregulated proteins did not show dose-dependent increase. In total, 55 deregulated proteins were common in both treatment doses. This represents 23% of all deregulated proteins. In five cases, the direction of the deregulation was opposite at these two radiation doses. The 55 common deregulated proteins were subjected to an in silico enrichment analysis (**Figure 8**) with the STRING web tool. Similar to the serum-derived EVs, the STRING enrichment analysis revealed that these proteins formed two clusters, both representing mainly defense or stress responses or responses to a stimulus.
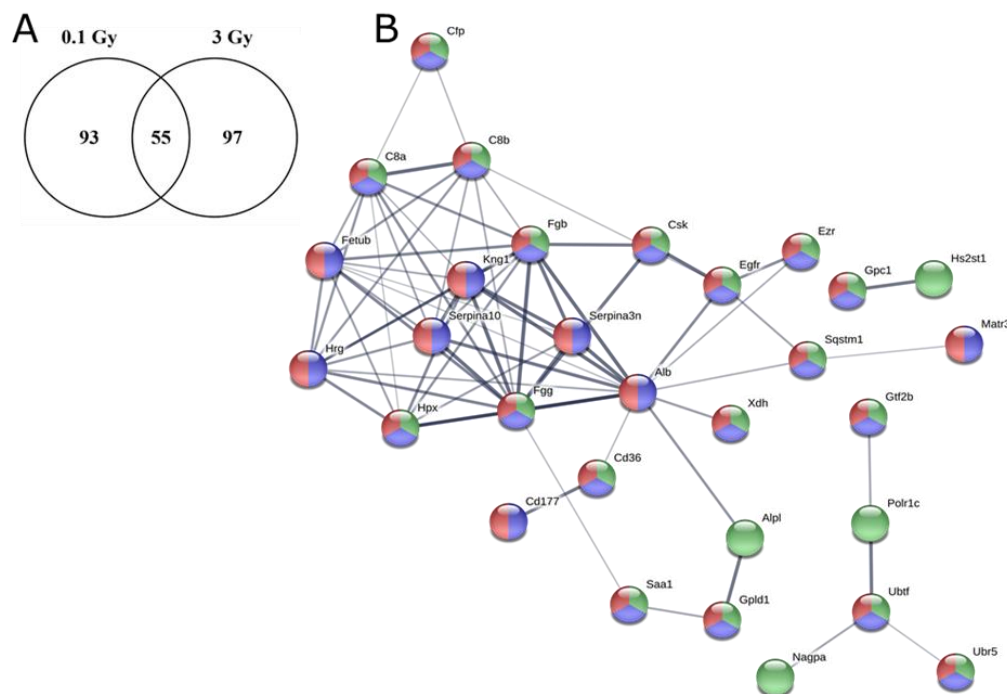
Figure 8. (A) A Venn diagram showing the number of deregulated proteins in bone marrow-derived EVs from mice treated with 0.1 Gy or 3 Gy TBI is shown. (B) STRING enrichment analysis of the 55 commonly deregulated pr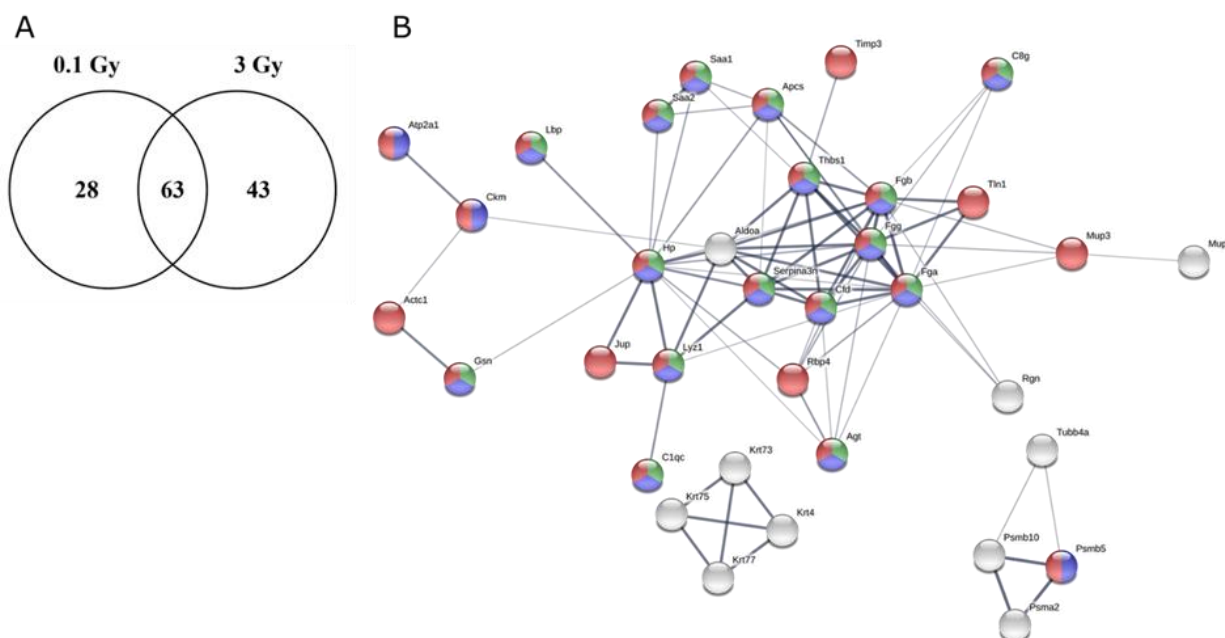oteins is illustrated. The proteins, belonging to defence response (GO:0006952, FDR 2.39 × 10-6, green), response to stress (GO:0006950, FDR 2.39 × 10-6, blue), and response to stimulus (GO:0050896, FDR 4.77 × 10-5, red), were all upregulated with the exception of UBTF.

In both EV types and at both radiation doses there were 15 common differentially regulated proteins. These proteins represented similar groups as seen with the previous analyses of serum or bone marrow-derived EVs, namely proteins responding to stress or stimulus or participating in the cellular defense. The shared deregulated proteins showed high level of clustering in the protein-protein interaction analysis (**Figure 9**). All proteins with the exception of angiotensin-converting enzyme (ACE) belonged to this cluster.

All deregulated proteins in both bone marrow-derived and serum-derived EVs were imported in the Ingenuity Pathway Analysis (IPA). The deregulated proteins from both EV types represented similar predicted upstream regulators and canonical pathways (**Figure 10**). The most important predicted upstream regulators were IL6, TGF beta 1, HNF4A (hepatocyte nuclear factor 4 alpha), and dimeric STAT3. The most important canonical pathways were acute phase response signalling, LXR/RXR signalling, FXR/RXR signalling, and coagulation system. This analysis indicates a possible role of both EV types in rapid reprogramming of protein expression and metabolism in response to radiation-induced inflammatory cytokine signalling.
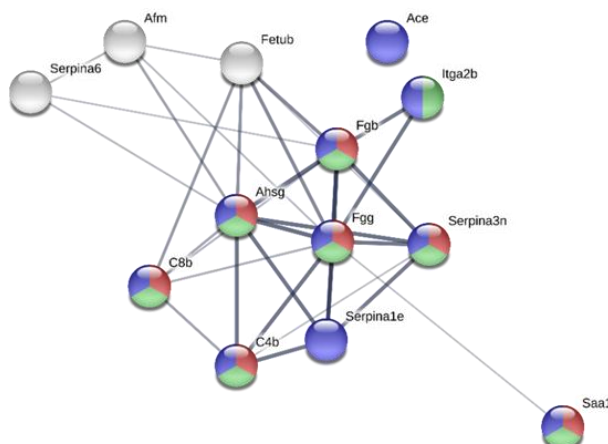
Figure 9. *STRING enrichment analysis of the common deregulated proteins in serum- and bone marrow-derived EVs. Proteins belonging to defence response (GO:0006952, FDR 5.39 × 10-5, red), response to stress (GO:0006950, FDR 0.0010, green), and response to stimulus (GO:0050896, FDR 0.0050, blue), are indicated.*
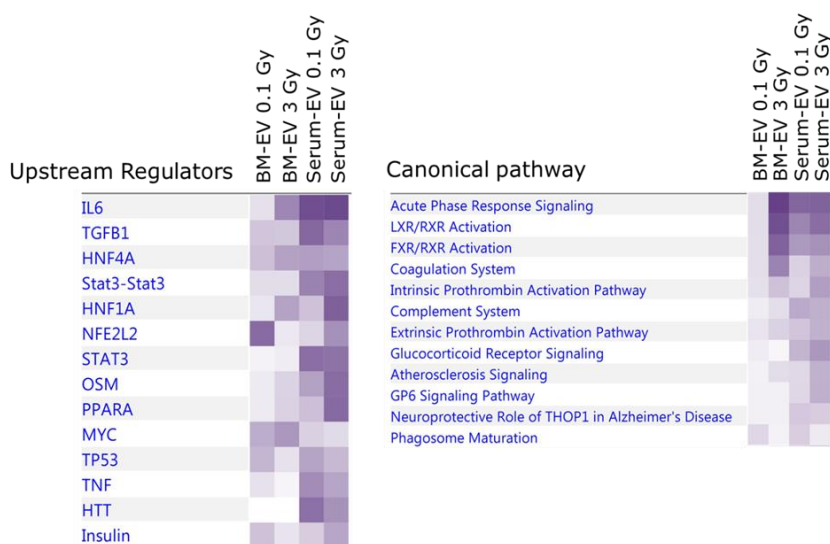
Figure 10. *The predicted upstream regulators and canonical pathways for the deregulated proteins identified in both bone marrow-derived and serum-derived EVs (the darker the color, the more accurate is the prediction). All colored boxes have a p-value of ≤ 0.05; white boxes have a p-value of ≥ 0.05 meaning no significant alteration compared to the sham-irradiation.*

In conclusion, a change in the proteome of the serum- and bone marrow-derived EVs was observed rapidly (24 h) after the mice were treated with 0.1 or 3 Gy TBI. No dose-dependent increase in the number of deregulated proteins was observed in either serum- or bone marrow-derived EVs. However, the number of common deregulated proteins between the two radiation doses was high, being 47% and 23% in serum- and bone marrow-derived EVs, respectively. In-silico protein–protein interaction analysis of the significantly differentially expressed proteins in either the serum- or bone marrow-derived EVs showed interconnected protein clusters representing mainly stress and acute phase response proteins. Moreover, similar pathways and upstream regulators were predicted for the serum and bone marrow-derived proteins.

III. Cellular and molecular mechanisms mediated by EVs

A. Phenotypical changes in the bone marrow subpopulations of EV-treated mice

We investigate acute and chronic effects of bone marrow EV transfer on the bone marrow subpopulations. This was done by three scenarios: either EVs isolated from irradiated animals were injected in naïve mice 24 hours after irradiation and effects were investigated 24 hours (24hours/24 hours), or 3 months later (24hours/3months) or EVs isolated from irradiated animals were injected in naïve mice 3 months after irradiation and effects were investigated 24 hours later (3months/24 hours). Mice irradiated only and investigated 3 months after irradiation were used as controls to study direct radiation effects in these latter two groups.

EV-mediated radiation effects were present only if EVs were isolated 24 hours after irradiation (scenarios 24hours/24hours and 24hours/3months). If EVs were isolated 3 months after irradiation (scenario 3months/24hours), no EV-mediated radiation effects were present in the bone marrow of EV-recipient mice.

The most important cell pool changes after EV injection can be summarized as follows:

- Acutely after irradiation and EV treatment (24hours/24 hours) total <u>haematopoietic stem cells</u> decreased both in the directly irradiated and EV-treated mice dose-dependently. 3 months after treatment a significant decrease in the total HSC subpopulation could only be seen in the directly irradiated mice after 3 Gy, while a dose-dependent decrease was seen in EV-treated mice.
- The fraction of <u>lymphoid progenitors</u> in the bone marrow decreased significantly only after high dose irradiation and only after treatment with EVs from mice irradiated with high dose. These changes were equally present acutely (scenario 24hours/24hours) and chronically (24hours/3months) after treatment.
- Acutely after irradiation changes were mild in the <u>myeloid progenitors</u>, both in the directly irradiated and EV-treated mice and interestingly 0.25 Gy had the strongest effect. Three months after irradiation myeloid cells decreased strongly after high dose irradiation and the same effects were seen if mice were injected with EVs from 3 Gy-irradiated animals (scenario 24 hours/3months).
- Acutely after irradiation a moderate but statistically highly significant increase was seen in the fraction of <u>erythroid precursors</u> after high dose irradiation. In mice, which received EVs from the directly irradiated animals, the fraction of erythroid precursors decreased significantly after low dose irradiation (0.1 and 0.25 Gy). Chronic effects were absent.
- Irradiation and EV treatment did not induce statistically significant changes in the pool of <u>megakaryocyte precursors</u> either acutely or chronically after irradiation and EV treatment.
- Both direct irradiation and EV-mediated bystander signals induced a significant reduction of the <u>mesenchymal stem cell</u> pool in the bone marrow after all doses acutely after treatment. Changes were not dose dependent. Three months after irradiation only high dose irradiation induced a moderate but significant reduction in the MSC pool. Chronic EV-mediated bystander effects were absent.

In conclusion, our data show that EVs isolated acutely after irradiation can transmit radiation-related signals in the bone marrow and significantly alter the proportion of the different subpopulations in the stem cell compartment. It is very important to highlight that radiation-related signals transmitted by EVs were persistent and could be detected even 3 months after irradiation. However, if EVs were isolated from the animals 3 months after irradiation, EVs could not transmit any bystander signal.

B. Changes in the apoptotic rate, proliferation index and DNA damage level of haematopoietic cells treated with EV

Apoptosis in the bone marrow:

Apoptosis was an early event both after direct irradiation and EV treatment. While direct irradiation led to a dose-dependent increase in the rate of apoptosis in most of the studied cell populations, EV effects were detectable only in certain cell subpopulations. The rate of apoptosis in HSCs increased strongly both in directly irradiated and EV-treated mice but only after high dose irradiation (**Figure 11A**). Apoptosis in the lymphoid progenitors increased dose-dependently after direct irradiation. EVs induced increase in apoptotic frequency only after high dose irradiation (**Figure 11B**).
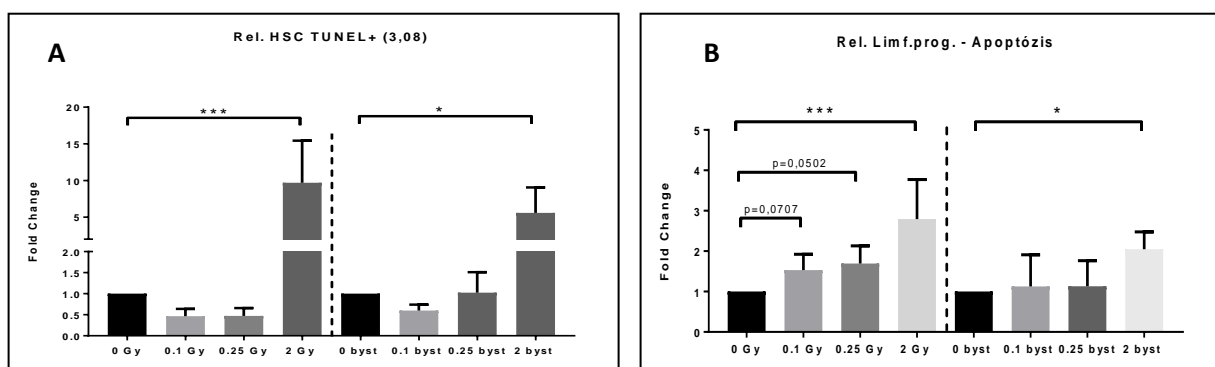
Figure 11: Evaluation of apoptosis in the different bone marrow subpopulations in the directly irradiated and EVC-treated mice. Mice were total-body irradiated with the indicated doses. EVs were isolated from the directly irradiated animals as described in the Methods and were injected in naïve mice. Both direct radiation effects and EV-mediated effects were investigated 24 hours after treatment. Bone marrow single cell suspensions were immune phenotypes as described above and apoptosis in the individual cell subpopulation were measured by flow cytometry using the TUNNEL assay. A: Apoptosis in the haematopoietic stem cells; B: Apoptosis in the lymphoid progenitors. Individual treatment groups comprised of a minimum of 6 animals. Error bars represent standard deviations. Statistical significance was evaluated by Student T-test. Statistically significant data points (p<0.05) are indicated by *.

Apoptosis and DNA damage in the spleen:

An immunohistochemistry analysis of mouse tissues derived from animals treated with total body irradiation was performed. First spleen tissue from leukaemic mice was compared to non-leukaemic mice.

Analysis covered quantification of double-stranded DNA breaks by γ-H2AX staining, proliferating cells detected by Ki-67 and apoptosis detected by cleaved Caspase 3. For morphological evaluation of the tissues, hematoxylin-eosin (HE) staining was performed in addition. The spleen morphology of the leukaemic mice was different to that observed in the non-leukaemic mice (**Fig. 12 A a-d**) with a more compact structure in leukaemic mice. The proportion of apoptotic (cleaved Caspase 3-positive) cells in the leukaemic mice was increased compared to that observed in the non-leukaemic mice (**Fig. 12 A e-h, B and C**). In contrast, the proportion of proliferating (Ki-67-positive) cells was not altered while DNA damage (gamma-H2AX) was slightly reduced in spleens derived from leukaemic mice.
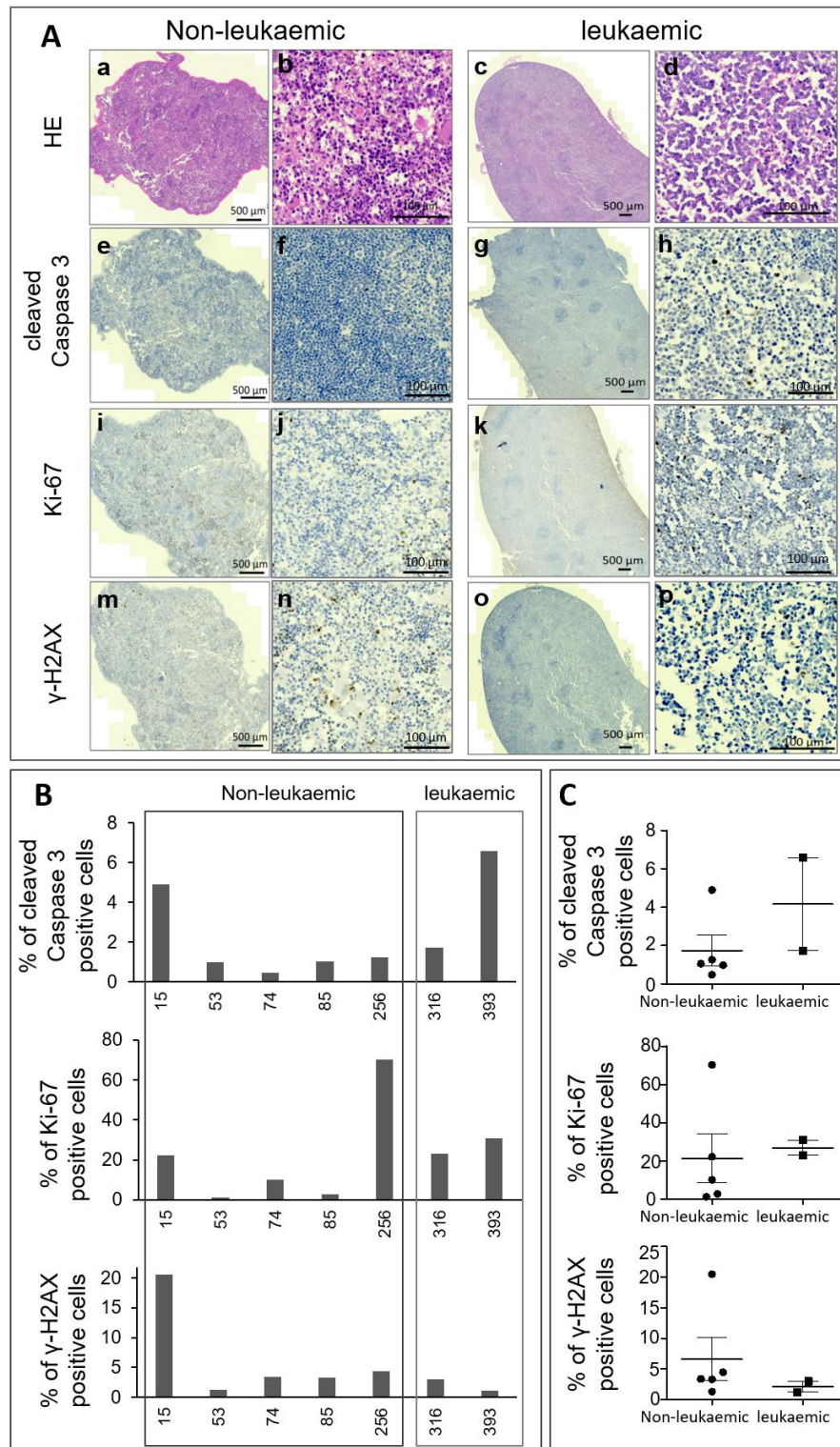
Figure 12: A Examples of HE staining and immunohistochemistry of leukaemic and non-leukaemic mice spleens. Tissue stained with Hematoxylin-eosin (HE) (a-d) and immunohistochemical staining with cleaved Caspase 3 (e-h), Ki-67 (i-l) and γ-H2AX (m-p). B Quantitative analysis of non-leukaemic and leukaemic mice of individual markers (Ki-67, cleaved Caspase 3 and γ-H2AX) was performed by the software QuPath V0. C Scatter plots showing distribution of cleaved Caspase 3, Ki-67 and γ-H2AX of non-leukaemic and leukaemic mice. Data are derived from 5 normal mice and 2 leukaemic mice.

C. Changes in the oxidative status and antioxidant system in the spleen of mice directly irradiated or treated with EVs

Previously we showed that EVs can transmit DNA damage signals in a bystander manner in the spleen. Therefore, we investigated whether these effects are due to the transmission of oxidative stress.

Gene expression changes in the antioxidant enzymes (SOD2, CAT, GSTs)

We found that direct exposure to 0.1 Gy did not affect the expression of any of the studied antioxidant enzymes in the spleen 24 hours after exposure, while as a result of high dose irradiation the expressions of SOD2 (superoxide dismutase 2, mitochondrial) and CAT (catalase) genes were reduced in the spleen, and expression of GSTs also showed a decreasing tendency, although it did not reach a level of significance. The expression of SOD2, CAT and GSTs did not change in the spleen 24 hrs after exposure to bone marrow-derived EVs of mice exposed to 0.1 Gy. In contrary, 24 hrs after exposure to bone marrow-derived EVs of mice exposed to high dose irradiation, the expression of all studied antioxidant enzymes (SOD2, CAT and GSTs) was significantly reduced (*Figure 13*).

These results suggest that EVs from irradiated cells may transfer signals that may reduce the expression of antioxidant enzymes, similarly as found in the directly irradiated tissue.
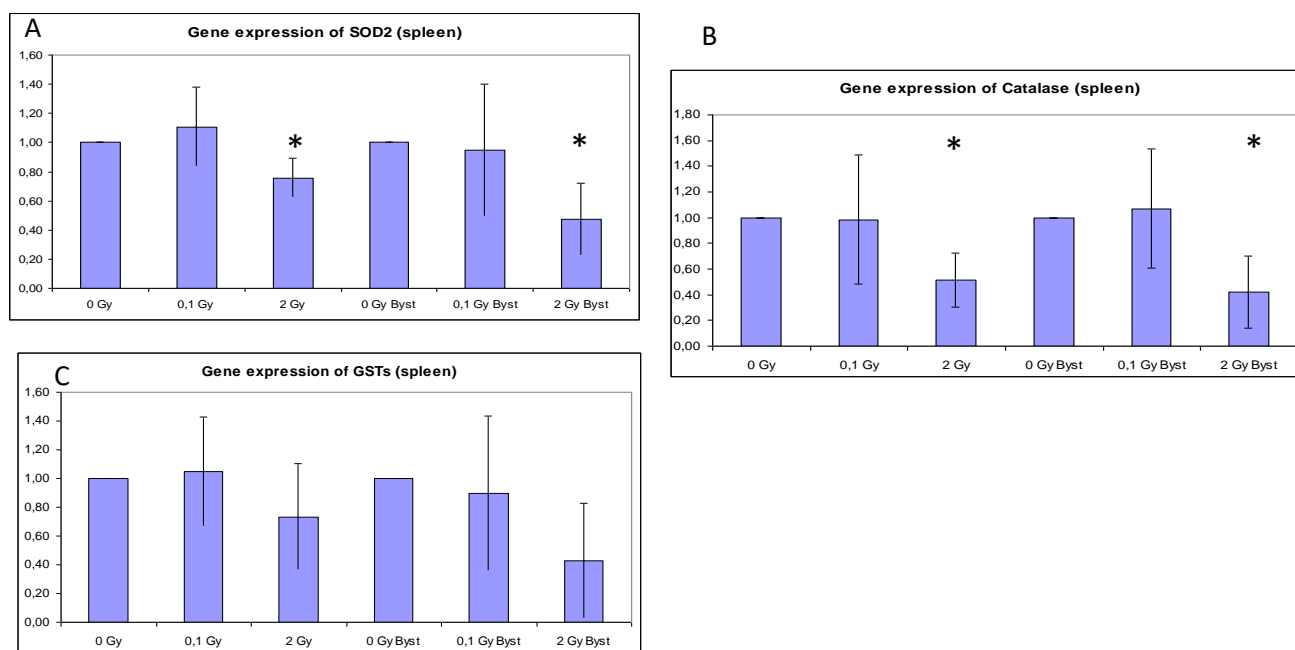
Figure 13. Average (± SD) relative gene expression of superoxide dismutase (A), catalase (B) and glutathione S-transferase enzyme (C) in the spleen of mice 24 hrs after exposure to irradiation or exposure to bone marrow-derived EVs of irradiated mice. 0 Gy and 0 Gy Byst were considered to be the baseline expression in the directly irradiated and bystander groups, respectively. N = 6

D. Changes in senescence markers in the spleen of mice directly irradiated or treated with EVs

We found that the expression of P16 (cyclin dependent kinase inhibitor 2A; Cdkn2a) gene, which at present is considered the most reliable senescence marker in the spleen did not change significantly 24 hours after exposure to low dose or after exposure to bone marrow-derived EVs of low dose irradiated mice, although a tendency for an elevated expression was observed. 24 hours after exposure to high dose we detected a highly significant elevation in the expression of P16 gene in the spleen. Similarly, expression of P16 gene showed a significant increase 24 hours after exposure to bone marrow-derived EVs of high dose irradiated mice (*Figure 14*).
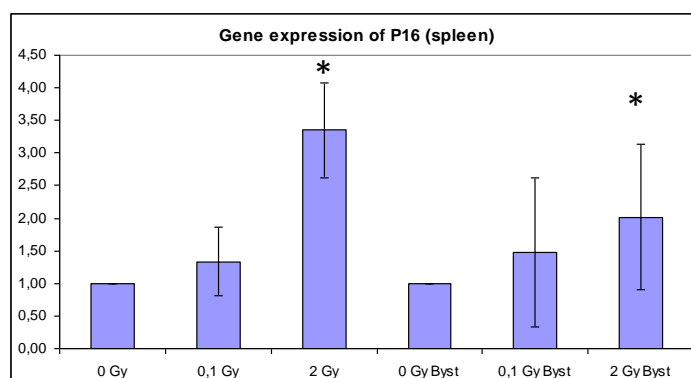
Figure 14. *Average (± SD) relative gene expression of P16 in the spleen of mice 24 hrs after exposure to irradiation or exposure to bone marrow-derived EVs of irradiated mice. 0 Gy and 0 Gy Byst were considered to be the baseline expression in the directly irradiated and bystander groups, respectively. N=6. Statistical significance was evaluated by Student T-test. Statistically significant data points (p<0.05) are indicated by *.*

E. The rate of EV uptake in the bone marrow and major EV acceptor cells

Our previous results indicated a differential effect of EVs in the different cellular subpopulations in the bone marrow. This suggests a differential uptake of EVs by the various cell types. Thus, we aimed at studying EV uptake in the bone marrow and to identify EV uptake rate by individual cell types.

BM single cell suspension derived from mice irradiated with low or high doses were incubated with EVs derived from mice irradiated with low or high doses. Regarding EV uptake by the unfractionated BM cell population we showed that:
-   if non-irradiated BM cells were co-cultured with irradiated EVs, a minor decrease in EV uptake was seen after incubation with EVs from 2 Gy-irradiated mice,
-   if irradiated BM cells were co-cultured with EVs isolated from non-irradiated mice, a major decrease in EV uptake was seen in the cells irradiated with 2 Gy;
-   if the two scenarios were combined, a further decrease was seen in the cells which were irradiated with 2 Gy and were co-incubated with EVs from mice irradiated with 2 Gy. The effect was synergistic.

Regarding the distribution of the different BM subpopulation within the fraction of cells which picked up the EVs we showed that:
-   irradiation of either the cells directly or the EVs had the greatest impact on the EV uptake of two cell populations: the erythroid precursors and the myeloid progenitors. The rate of EV-acceptor erythroid progenitors decreased either after direct irradiation or after incubation with EVs from irradiated animals. In contrast, the rate of EV-acceptor myeloid progenitors strongly increased if either were originating from mice irradiated with 2 Gy or if were incubated with EVs originating from 2 Gy-irradiated mice.

This indicates that both irradiation of acceptor cells and irradiation of EVs influence EV uptake but irradiation of acceptor cells has a stronger effect.

IV. Identification of IR-related and leukaemia risk-associated biomarkers in human leukaemia patients subjected to total body irradiation

Patients with leukaemia (AML, ALL) were conditioned for stem cell transplantation at the Department of Radiotherapy, GUF, and blood samples were collected from 11 leukaemic patients before (d0) and after TBI with 2 x 2 Gy (d1) while 11 healthy donors served as controls. Various commercial kits (ExoQuick, Exo Quick ULTRA) were tested to isolate the EVs from human serum but the purity of the recovered EVs was not suitable for proteomic analysis. Consequently, an

ultracentrifugation protocol was established and EVs were subjected to WB and FC for quality control. These indicated detection of typical EV markers (CD9, CD81 and TSG-101) and suitability of these particles for proteomic analyses to be performed at HMGU.

A. Patients' and healthy donors' characteristics

In total, EVs were isolated, before and after irradiation with 2 x 2 Gy, from 12 leukaemic patients while the second sample of one patient was not assessable due to its bad health state. The median age of females was 42.8 years (n=5) and of males 53.4 years (n=7) (*Table 9*). 40 % of women suffered from acute myeloid leukaemia (AML) and 60 % from acute lymphoid leukaemia (ALL) (*Table 9*) while 85.7 % of all males suffered from AML and 14.3 % from ALL (*Table 9*). In addition, EVs were also isolated from 11 age matched healthy donors. The median age of female donors was 41.2 years (n=5) and of males 43.7 years (n=6).

Donor	Sex	n	mean age/years	acute myeloid leukaemia/%	acute lymphoid leukaemia/%
Leukaemic patients	female	5	42.8±17	40.0	60.0
	male	7	53.3±8	85.7	14.3
Healthy donors	female	5	41.2±11	N/A	
	male	6	43.7±11		

Table 9. Patients and healthy donors characteristics

B. Characterization of the EVs

Exemplary immunoblot analyses of EV markers TSG-101, CD81 and CD9 and the ER marker Calnexin of three patients before (d0) and after irradiation (d1) and of healthy donors revealed detection of CD9 in all patients and healthy donors and, as expected, lack of Calnexin detection in the EVs. By contrast, Tumor susceptibility gene 101 (TSG-101) detection was mainly restricted to patient-derived EVs. In flow cytometry analysis, we confirmed the positive signals for CD9 in healthy donors and leukaemic patients. In addition and in contrast to Western blot analyses, in patient-derived EVs a positive signal for CD81 was detected in both, leukaemic patients and healthy donors. Next, the EVs from human serum were distributed to the partners. In total, 40 µg per sample (leukaemic patients and healthy donors) were sent to HMGU to perform proteomic analysis and to Arraystar (Rockville, USA) to perform miRNA analyses.

In conclusion, the results of the Western blot and flow cytometry analysis indicate that isolation protocol by ultracentrifugation for EVs from serum was successful as detection of typical EV markers such as CD9, CD81 and TSG-101 was suitable in both leukaemic patients and healthy donors.

C. Proteomic analysis of EVs cargo from leukaemic patients and healthy donors

In this study, 255 proteins were identified when 1 % FDR (false discovery rate) was applied, amongst which 199 proteins were identified with at least two unique peptides. A clustering in principal component analysis (PCA) for healthy controls was observed (*Figure 15*) based on intensities of the identified proteins.
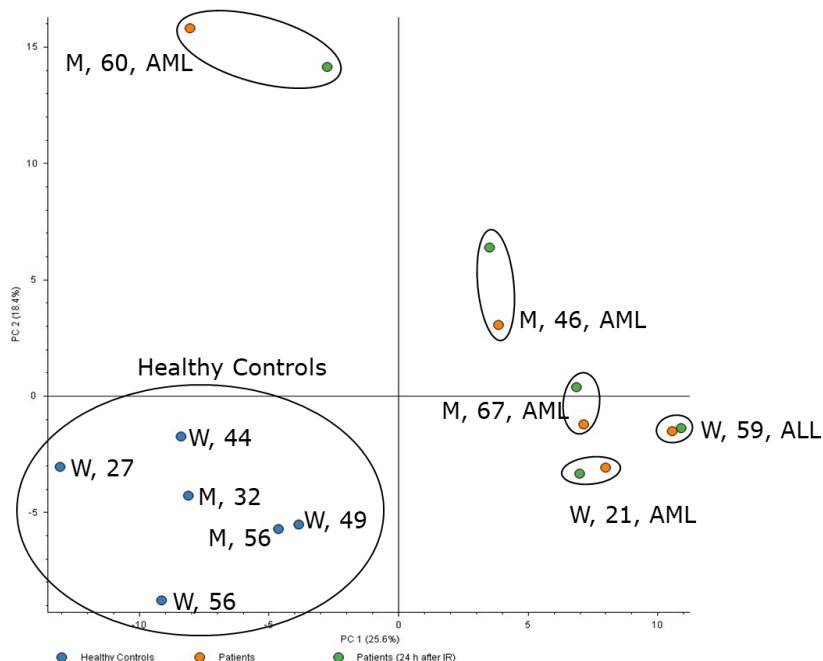
Figure 15. Principal component analysis (PCA) based on all proteomic features of serum-derived EVs from healthy controls and leukemic patients. Clustering of healthy control samples (blue) is observed. The sex (M/W), age, and the type of leukaemia if relevant is indicated. The PCA coordinates for the same patient before (orange) and after exposure to IR (green) were not markedly changed, indicating only small alterations in the EV cargo due to irradiation.

Protein abundances in patient EVs before exposure to IR were compared with healthy controls. Six downregulated and 21 upregulated proteins were observed in the patient EVs in comparison to the EVs from healthy donors. The significantly deregulated proteins were subjected to an in silico enrichment analysis with the STRING web tool. A clear clustering of all except two proteins was shown (*Figure 16*). A great majority (96%) of these proteins were involved in cellular defense (20/27), response to stress (22/27) or response to stimulus (26/27).
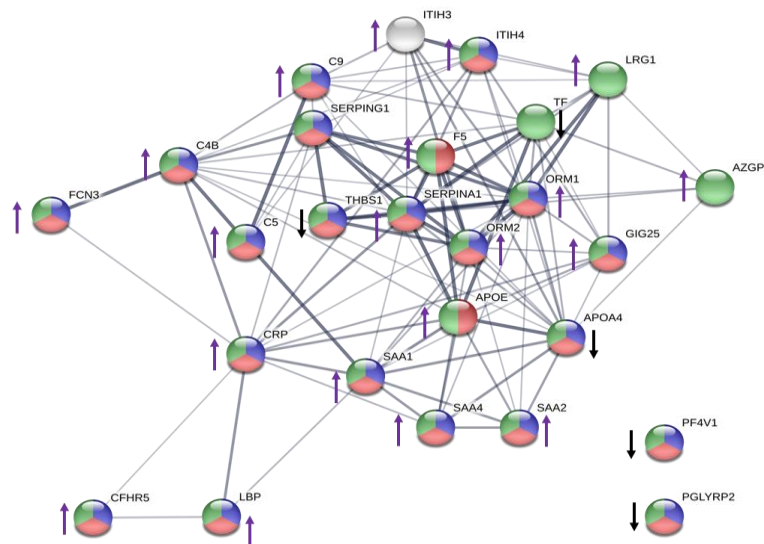
Figure 16. Deregulated proteins identified in serum-EVs from leukemic patients (d0-EVs) compared to healthy controls. The proteins with most 'counts' in the gene set belonging to defense response (GO:0006952, FDR 1.15 × 10-16, blue), response to stress (GO:0006950, FDR 1.15 × 10-11, red) and response to stimulus (GO:0050896, FDR 1.11 × 10-7, green) were present. Up- and downregulated proteins are marked with purple and black arrows, respectively.

To evaluate radiation biomarkers in EVs, the protein abundances in patient EVs 24 h after irradiation (d1-EV) were compared with EVs of the same patient before irradiation (d0-EV). Fourteen proteins that were upregulated and 23 downregulated proteins (fold change +1.3) in at least three out of five patients were subjected to in silico enrichment analysis (*Figure 17*). This analysis showed two distinct clusters of proteins (*Figure 17*). The big cluster consisted of 30 proteins and the small one of 5 proteins. Only two proteins had no interaction with any other deregulated protein. Also in this case most of the proteins belonged to cellular defense, stress response or response to stimulus as indicated in the *Figure 17*.
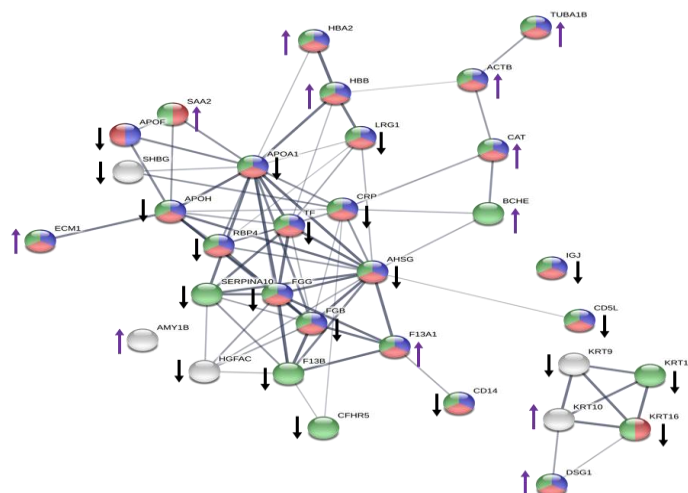
Figure 17. *Deregulated proteins observed in serum-EVs in at least three out of five patients after irradiation. The proteins with most 'counts' in gene set belonging to transport (GO:0006810, FDR 1.15 × 10-11, blue), localization (GO:0051179, FDR 3.01 × 10-5, red), and response to stimulus (GO:0050896, FDR 7.14 × 10-5, green) were present. Up- and downregulated proteins are marked with purple and black arrows respectively.*

There were four proteins commonly deregulated in both serum-EVs from patients (d0-EV) compared to healthy controls and serum-EVs from patients after IR (d1-EV) compared to before radiation (d0-EV). These are shown in *Table 10*.

Accession	Protein Description	Deregulation	
		Patients-EV/ Healthy-EV	Patients (d1-EVs/d0-EVs)
P02787	Serotransferrin [OS=Homo sapiens]	Down	Down
P02750	Leucine-rich alpha-2-glycoprotein [OS=Homo sapiens]	Down	Up
Q9BXR6	Complement factor H-related protein 5 [OS=Homo sapiens]	Down	Up
P02741	C-reactive protein [OS=Homo sapiens]	Down	Up
P0DJI9	Serum amyloid A-2 protein [OS=Homo sapiens]	Up	Up

*Table 10*. *List of common deregulated proteins between serum-EVs from leukaemic patients compared to healthy controls and in the serum-EVs 24 h after IR in leukaemic patients.*

In conclusion, markers of radiation exposure in serum-derived EVs were investigated in humans. Serum-derived EVs, before and after total body irradiation, were analysed for their protein content. Although the healthy controls showed clustering independent of the age or sex in the PCA based on the EV protein intensities, the PCA showed no marked clustering between the leukemic patients. The reason for this is unknown and more samples are needed to investigate this. Accordingly, significantly deregulated proteins could not be identified when the EVs of all the patients (d0-EVs) were treated as one group and compared against d1-EVs of all patients. Instead, the EVs from the same patient before and after irradiation were compared. Only those proteins were considered deregulated that showed same direction of expression change in at least three out of five patients. Most of the deregulated proteins were involved in localisation, transport and response to stress.

D. MiRNA analysis of EVs cargo from leukaemic patients and healthy donors

The miRNA from EVs from healthy donors was isolated with the RNeasy Mini Kit (QIAGEN) and should be subjected to a nCounter assay (nanoString Technologies). However, these establishing steps revealed that miRNA concentration from human serum samples were too low for analyses with this technology. As an alternative, we decided to change methodology to a NGS approach offered by a commercial company, Arraystar. According to the company's recommendation, miRNAs were isolated from blood samples of healthy donors and leukaemic patients before (d0) and after (d1) irradiation using miRNeasy Mini Kit (QIAGEN) designed to extract total RNA including microRNAs. The RNA yield covered 3.2 to 12 ng/µl. The miRNA sequencing was performed by Arraystar, using an Illumina NextSeq 500 system.

Samples covering in total three samples of healthy donors and three samples from patients with and without irradiation were transferred to the company and sequenced. The sequencing quality score revealed sufficient quality for subsequent data analysis in all samples. Data analysis after sequencing was performed with the software miRDeep29 to quantify known miRNA and predict novel miRNAs. Additionally, differentially expressed miRNA were filtered using R package edgeR10,11, hierarchical clustering and miRNA target prediction was performed by targetscan and additional methods. Gene ontology (G) and KEGG pathway analysis was done based on the top 10 differentially expressed miRNAs.

Differential miRNA expression in serum-derived EVs of leukaemic patients vs. healthy controls

Sequencing analysis of miRNAs in EVs derived from serum of leukaemic patients and healthy donors resulted in 440 upregulated, 242 not differentially expressed and 236 downregulated miRNAs, displayed as a Scatter Plot (*Figure 18*). Of these, 44 miRNAs were significantly (p<0.05) upregulated (fold change ≥2.5) (*Table 11*) and 10 were significantly downregulated (fold change≤0.35) (*Table 12*).
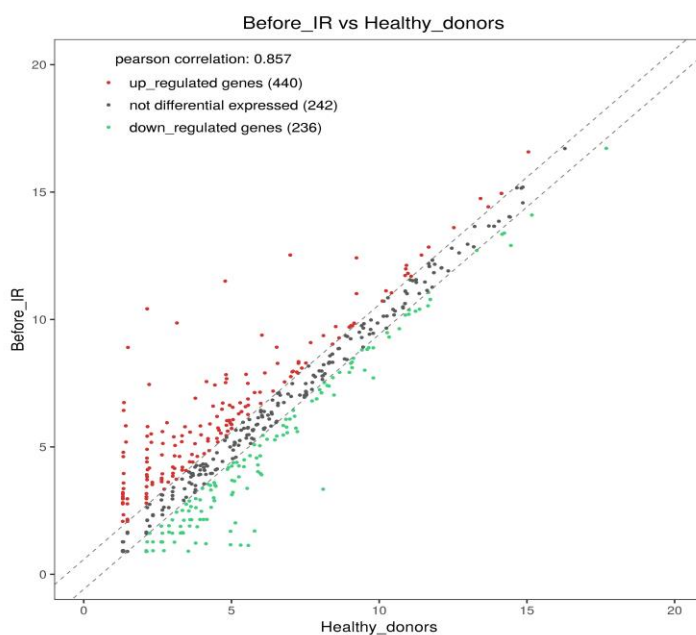
Figure 18. Scatter Plot of differentially expressed miRNAs in EVs of leukaemic patients (Before_IR) compared to healthy donors (Healthy_donors). The values of X and Y axes in the Scatter Plot are the averaged counts per million reads (CPM) values of each group (log2 scaled). miRNAs above the top line (red dots, upregulation) or below the bottom line (green dots, downregulation) indicate more than 1.5-fold change between the two compared groups. Grey dots indicate non-differentially expressed miRNAs.

Mature miRNA ID	Arm	Log$_2$fc	Fold change	p value	q value
hsa-miR-509-3p	3p	8.27	309.27	0.00006	0.00976
hsa-miR-4497	5p	7.75	215.96	0.00000	0.00166
hsa-miR-506-3p	3p	7.41	169.76	0.02762	0.58973
hsa-miR-4492	5p	6.90	119.34	0.00024	0.02455
hsa-miR-509-3-5p	5p	6.72	105.33	0.00935	0.27932
hsa-miR-508-3p	3p	6.71	104.62	0.00136	0.09621
hsa-miR-1269a	5p	6.32	80.07	0.00196	0.12752
hsa-miR-1469	5p	5.99	63.76	0.00547	0.23925
hsa-miR-141-5p	5p	5.95	61.91	0.00671	0.24652
hsa-miR-513c-5p	5p	5.91	60.13	0.00751	0.26502
hsa-miR-514a-3p	3p	5.54	46.53	0.01680	0.44068
hsa-miR-195-3p	3p	5.38	41.59	0.00010	0.01135
hsa-miR-576-3p	3p	5.36	41.17	0.02600	0.58212
hsa-miR-7704	5p	5.24	37.70	0.00002	0.00534
hsa-miR-202-3p	3p	5.23	37.63	0.03735	0.66520
hsa-miR-522-3p	3p	5.22	37.38	0.03797	0.66520
hsa-miR-548ah-3p	3p	5.09	34.06	0.04831	0.76465
hsa-miR-548p	5p	5.09	34.06	0.04831	0.76465
hsa-miR-615-3p	3p	5.08	33.87	0.00038	0.03463
hsa-miR-509-5p	5p	4.41	21.19	0.00934	0.27932
hsa-miR-92b-5p	5p	3.64	12.44	0.00938	0.27932
hsa-miR-10400-5p	5p	3.41	10.62	0.00046	0.03876
hsa-miR-200a-5p	5p	3.36	10.24	0.00010	0.01135
hsa-miR-508-5p	5p	3.27	9.67	0.02761	0.58973
hsa-miR-135a-2-3p	3p	3.23	9.37	0.03829	0.66520
hsa-miR-200c-3p	3p	3.19	9.11	0.00000	0.00166
hsa-miR-202-5p	5p	3.13	8.78	0.00618	0.24652
hsa-miR-1301-3p	3p	3.13	8.77	0.02051	0.49547
hsa-miR-4488	5p	3.02	8.11	0.00114	0.08733
hsa-miR-135b-5p	5p	2.99	7.94	0.00236	0.12752
hsa-miR-664a-5p	5p	2.94	7.66	0.03221	0.62765
hsa-miR-4508	5p	2.84	7.17	0.00229	0.12752
hsa-miR-511-5p	5p	2.72	6.60	0.00335	0.16198
hsa-miR-155-5p	5p	2.38	5.21	0.00216	0.12752
hsa-miR-708-3p	3p	2.35	5.11	0.00648	0.24652
hsa-miR-760	5p	2.22	4.67	0.03840	0.66520

Mature miRNA ID	Arm	Log₂fc	Fold change	p value	q value
hsa-miR-1260a	5p	2.02	4.04	0.04973	0.77103
hsa-miR-429	5p	1.94	3.83	0.03130	0.62765
hsa-let-7e-5p	5p	1.78	3.44	0.00606	0.24652
hsa-miR-320d	5p	1.77	3.42	0.03292	0.62765
hsa-miR-141-3p	3p	1.72	3.29	0.03052	0.62765
hsa-miR-122-5p	5p	1.53	2.88	0.02035	0.49547
hsa-miR-28-3p	3p	1.41	2.66	0.04689	0.76465
hsa-miR-99a-5p	5p	1.32	2.50	0.02596	0.58212

Table 11. *Significantly upregulated miRNAs in EVs from leukaemic patients vs. healthy donors. Log2fc ≥1.32, p value cut-off <0.05, q value cut-off ≤1. Mature miRNA ID, ID of mature miRNA; Arm, arm of miRNA (3p/5p); log2fc, log2 scaled fold change; Fold change, 2test_CPM-control_CPM; p value, F-statistic p value; q value, FDR-adjusted p value; CPM, counts per million reads.*

Mature miRNA ID	Arm	Log₂fc	Fold change	p value	q value
hsa-miR-660-3p	3p	-5.57	0.02	0.02216	0.52171
hsa-miR-10527-5p	5p	-5.37	0.02	0.03350	0.62765
hsa-miR-592	5p	-4.44	0.05	0.01002	0.28754
hsa-miR-369-3p	3p	-4.17	0.06	0.01978	0.49547
hsa-miR-323b-3p	3p	-4.08	0.06	0.00493	0.22646
hsa-miR-4446-3p	3p	-3.81	0.07	0.04557	0.76056
hsa-miR-431-5p	5p	-3.28	0.10	0.04485	0.76056
hsa-miR-223-3p	3p	-2.10	0.23	0.00284	0.14497
hsa-miR-184	5p	-1.55	0.34	0.00943	0.27932
hsa-miR-31-5p	5p	-1.50	0.35	0.03227	0.62765

Table 12. *Significantly downregulated miRNAs in EVs from leukaemic patients vs. healthy donors. Log2fc ≤-1.50, p value cut-off <0.05, q value cut-off ≤1. Mature miRNA ID, ID of mature miRNA; Arm, arm of miRNA (3p/5p); log2fc, log2 scaled fold change; Fold change, 2test_CPM-control_CPM; p value, F-statistic p value; q value, FDR-adjusted p value; CPM, counts per million reads.*

Next, hierarchical Clustering analysis was performed using significant differentially expressed miRNAs in leukaemic patient- compared to healthy donor-derived EVs (**Figure 19**). Each row indicates a miRNA and each column represents a sample. The red color indicates higher expression values, the green colour indicates lower expression values.
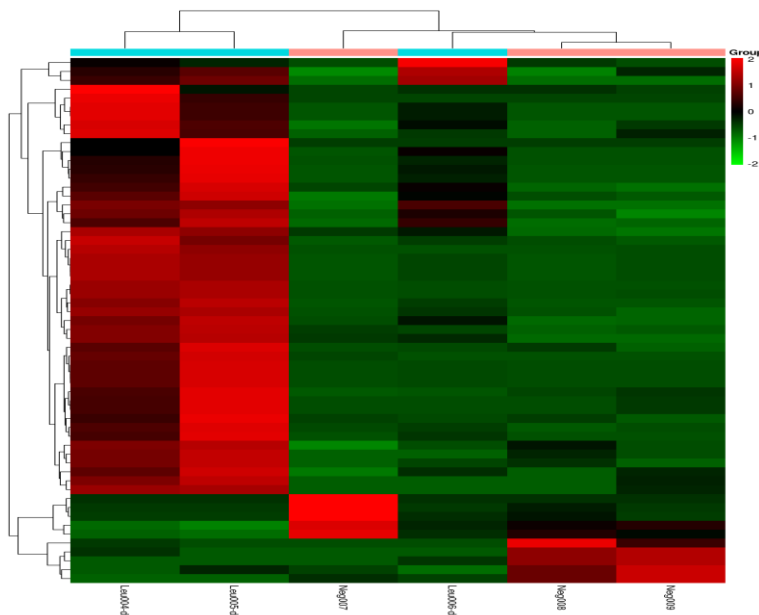
Figure 19*. Heatmap and cluster dendrogram of the EV miRNA sequencing data from non-irradiated leukaemic patients and healthy donors. Hierarchical Clustering was performed using differentially expressed miRNAs in serum-derived EVs from leukaemic patients (Leu004-06-d0) vs. healthy donors (Neg007-009).*

KEGG pathway analysis based on the Kyoto Encyclopedia of Genes and Genomes database revealed Transcriptional misregulation in cancer [hsa05202], Hedgehog signalling pathway [hsa04340] and Pathways in Cancer [hsa05200] amongst the most significantly affected pathways by miRNAs upregulated in leukaemic patients vs. healthy controls (***Figure 20***). However, acute myeloid leukaemia pathway [hsa05221] is also affected (p = 0.015). Most significantly affected pathways by downregulated miRNAs when comparing EV miRNA cargo of leukaemic patients in comparison to healthy donors revealed mineral absorption, pancreatic secretion and calcium signalling pathways to be amongst the top 10 significant pathways (***Figure 21***).
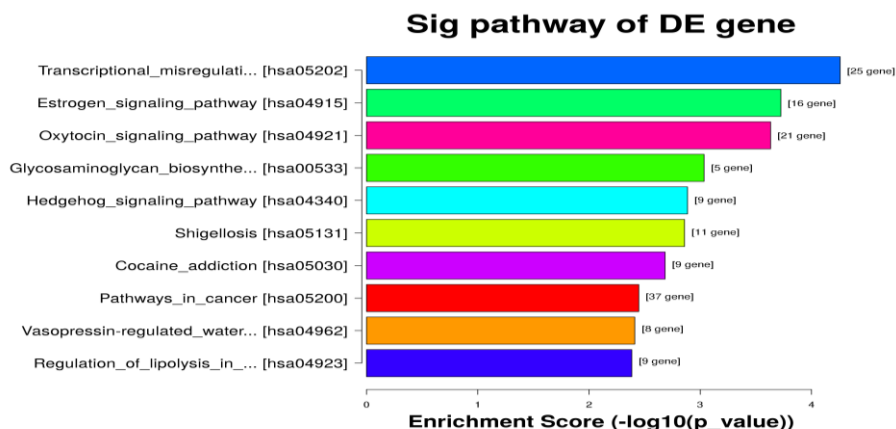

Figure 20*. Top 10 significant pathways of the gene targets of the upregulated miRNAs in leukaemic patient's EVs vs. healthy donors. Ordered from top to bottom by p value, with the most significant pathway on the top. The p values calculated by Fisher's exact test are used to estimate the statistical significance of the enrichment of the pathways between the two groups.*

Figure 21. *Top 10 significant pathways of the gene targets of the downregulated miRNAs in leukaemic patient's EVs vs. healthy controls. Ordered from top to bottom by p value, with the most significant pathway on the top. The p values calculated by Fisher's exact test are used to estimate the statistical significance of the enrichment of the pathways between the two groups.*
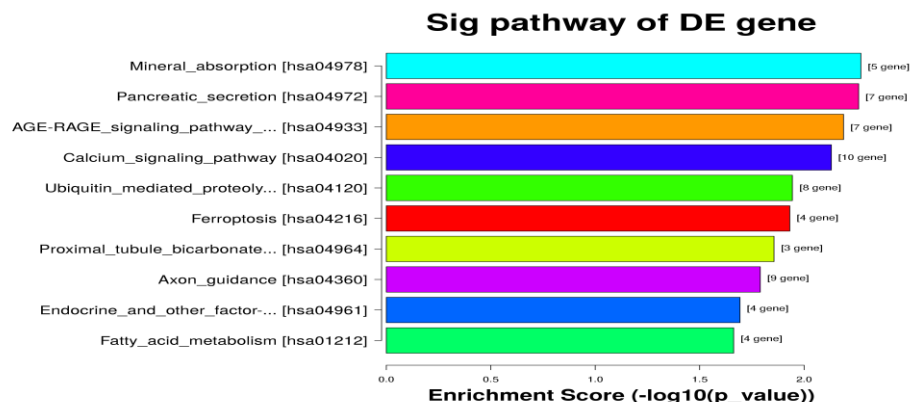
Gene ontology analysis of radiation-induced miRNAs identified target genes involved in transcription factor activity and sequence-specific DNA binding, transcriptional regulation by RNA polymerase II and Calcium ion binding (***Table 13***). MiRNAs, which are downregulated in leukaemic patients are impacting on genes involved in protein, peptide and amide binding according to gene ontology analysis (***Table 14***).

miRNA target genes – Biological process
- Multicellular organism development
- Nervous system development
- Positive regulation of metabolic process
miRNA target genes – Cellular component
- Cytoplasm
- Cell
- Cell projection
miRNA target genes – Molecular function
- Transcription factor activity, RNA polymerase II proximal promoter sequence-specific DNA binding
- RNA polymerase II regulatory region sequence-specific DNA binding
- Calcium ion binding

Table 13. *Gene ontology analysis of the leukaemia-induced miRNAs. Top 3 terms are shown of each category.*

miRNA target genes – Biological process
- Golgi organization
- Anatomical structure morphogenesis
- Endomembrane system organization
miRNA target genes – Cellular component
- Membrane-bounded organelle
- Golgi cis cisterna
- Intracellular membrane-bounded organelle
miRNA target genes – Molecular function
- Protein binding
- Peptide binding
- Amide binding

Table 14. *Gene ontology analysis of miRNAs downregulated in leukaemic patients. Top 3 terms are shown of each category.*

Differential miRNA expression in serum-derived EVs before and after total body irradiation of leukaemic patients

Comparison of miRNA expression in serum-derived EVs from three 2 x 2 Gy total body irradiated leukaemic patients (d1) with EVs, isolated from the same patients before irradiation (d0) revealed 293 upregulated, 308 not differentially expressed and 360 downregulated miRNAs (***Figure 22***). Only six miRNAs were significantly (p<0.05) upregulated (fold change≥2.5) (***Table 15***) and none were significantly downregulated.
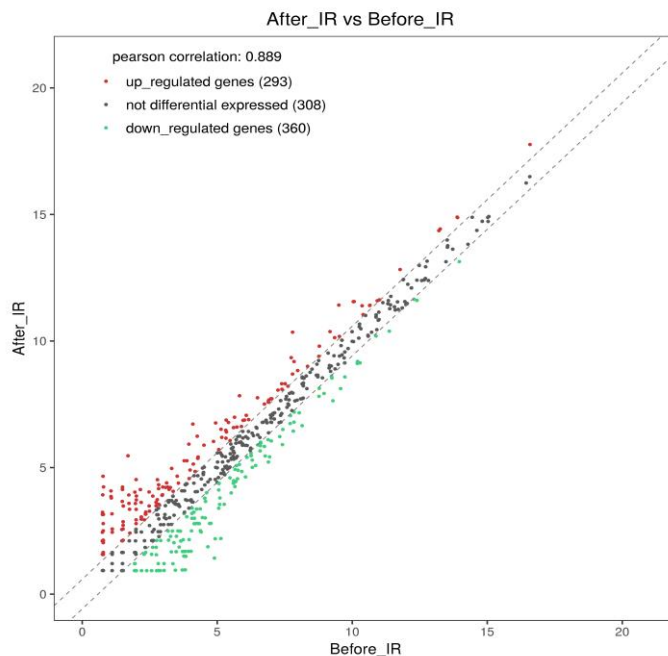

Figure 22. *Scatter Plot of differentially expressed miRNAs in EVs of leukaemic patients after total body irradiation (After_IR) compared to non-irradiated patients (Before_IR). The values of X and Y axes in the Scatter Plot are the averaged counts per million reads (CPM) values of each group (log2 scaled). miRNAs above the top line (red dots, upregulation) or below the bottom line (green dots, downregulation) indicate more than 1.5-fold change between the two compared groups. Grey dots indicate non-differentially expressed miRNAs.*

Mature miRNA ID	Arm	Log$_2$fc	Fold change	p value	q value
hsa-miR-3940-3p	3p	5.66	50.59	0.0283	1
hsa-miR-942-5p	5p	3.77	13.66	0.0300	1
hsa-miR-4732-5p	5p	2.62	6.16	0.0240	1
hsa-miR-16-2-3p	3p	2.56	5.89	0.0041	1
hsa-miR-501-3p	3p	2.01	4.04	0.0333	1
hsa-miR-144-3p	3p	1.92	3.77	0.0216	1

Table 15. *Significantly upregulated miRNAs after irradiation of leukaemic patients. Log2fc ≥1.32, p value cut-off <0.05, q value cut-off ≤1. Mature miRNA ID, ID of mature miRNA; Arm, arm of miRNA (3p/5p); log2fc, log2 scaled fold change; Fold change, 2test_CPM-control_CPM; p value, F-statistic p value; q value, FDR-adjusted p value; CPM, counts per million reads.*

KEGG pathway analysis of significantly affected pathways affected by miRNAs upregulated by irradiation of leukaemic patients revealed p53, RNA degradation, drug metabolism, FoxO and melanoma signalling pathways to be involved (*Figure 23*). Gene ontology analysis of radiation-induced miRNAs identified target genes mainly involved in transcriptional regulation by RNA polymerase II (*Table 16*).
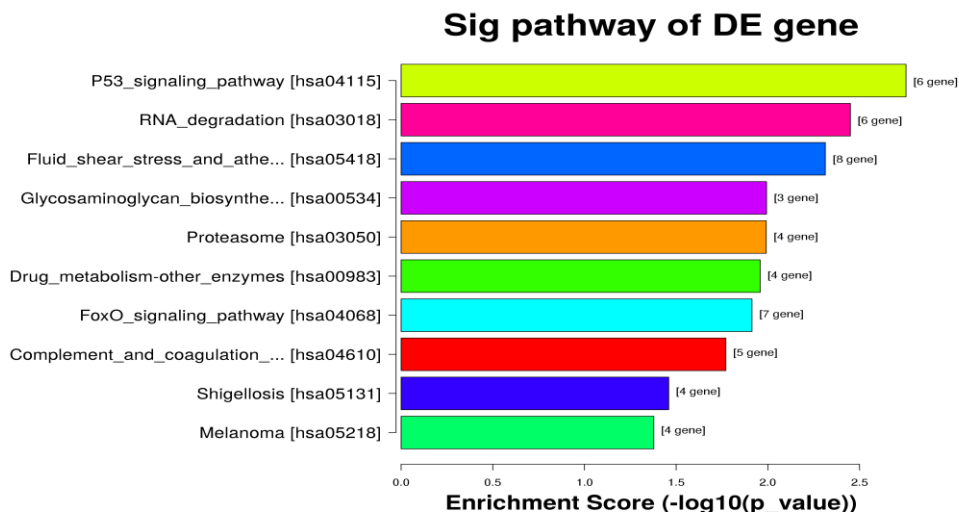

Figure 23. *Top 10 significant pathways of the gene targets of the upregulated miRNAs in EVs before and after irradiation of leukaemic patients. Ordered from top to bottom by p value, with the most significant pathway on the top. The p values calculated by Fisher's exact test are used to estimate the statistical significance of the enrichment of the pathways between the two groups.*

miRNA target genes – Biological process
- Regulation of transcription by RNA polymerase II
- Nervous system development
- Regulation of RNA metabolic process
miRNA target genes – Cellular component
- Nucleus
- Membrane-bound organelle
- Intracellular
miRNA target genes – Molecular function
- RNA polymerase II regulatory region sequence-specific DNA binding
- RNA polymerase II regulatory region DNA binding
- Transcription regulatory region sequence-specific DNA binding

Table 16. *Gene ontology analysis of the radiation-induced miRNAs in leukaemic patients. Top 3 terms are shown of each category.*

In conclusion, miRNA sequencing analysis of serum-derived EVs from leukaemic patients in comparison to healthy donors revealed a panel of 44 significantly and highly upregulated miRNAs with the highest upregulated one, hsa-miR-509-3p, showing a 309-fold upregulation in patients. Genes regulated by these miRNAs are mainly involved in cancer-related pathways, including acute myeloid leukaemia. Only 10 miRNAs were downregulated in EVs from leukaemic patients. These miRNAs are involved in regulation of pathways, which have functions in mineral absorption and calcium signalling. Gene ontology analysis revealed leukaemia-induced miRNA target genes involved in transcriptional regulation processes

mediated by RNA polymerase II, while downregulated miRNA target genes were impacting on genes functionally related to protein, peptide and amide binding and involved in biological processes like golgi or membrane organization.

In contrast, total body irradiation of leukaemic patients with 2 x 2 Gy revealed only 6 significantly upregulated miRNAs in serum-derived EVs and no significantly downregulated miRNAs. Hsa-miR-3940-3p showed 51-fold upregulation after irradiation and might serve as a marker for radiation exposure. Pathways affected by radiation-induced miRNAs include p53, RNA degradation, drug metabolism, FoxO and melanoma signalling pathways. Most of the genes, regulated by differentially expressed miRNAs, were involved in RNA polymerase II-related transcriptional processes, similar to leukaemia-induced miRNAs.

Overall, the presented data revealed highly specific regulation of miRNAs in leukaemic patients and after irradiation, which might serve as biomarkers for leukaemia and radiation exposure.

V. Education and training activites, exploitation of the results

Project-related E&T activities included the academic education of two PhD students, two MSc students and three BSc students partly financed by the project. Young scientists participated at national and international training courses on diverse topics such as basic molecular biology techniques, proteomic and mass spectrometry data set and statistical analysis, as well as radiobiology.

Two educational events were specifically initiated and/or organised by the project. The Young Scientist´s Session during the European Radiation Protection Week (ERPW), Rovinj, Croatia, 5.10.2018 gave students the possibility to exercise their presentation skills in front of a large audience. We especially welcomed not only the peers but also the more experienced participants to give the presenters scientific questions, comments, and advice. Fourteen students gave a 15 min presentation each to an audience of around 60 attendees.

The training course "Essentials of radiation leukaemogenesis" was organised at CRCE (Public Health England, Oxfordshire, UK), 20th – 23th January 2020. The aim of the course was to provide information about the processes behind radiation-induced acute myeloid leukaemogenesis, including the key molecular and genetic events, risk factors and modifiers of risk. Ten participants, most of them senior scientists from different institutions around Europe, attended the training course which consisted of a theoretical and practical part.

Altogether, 39 conference presentations were prepared and presented by project partners at 10 different national and 13 different international meetings. Importantly, a focus was placed to disseminate project results outside the radiation research community as well, which led to poster and oral presentations at the annual meetings of the International Society for Extracellular Vesicles and at national and international cancer conferences. So far, project results were published in three scientific papers, 1 publication has just been submitted and it is under evaluation and further three joint papers are in preparation. Undoubtedly, the most important dissemination activity was the satellite meeting organized during the International Congress on Radiation Research in Manchester, UK, 25-29 August, 2019. This meeting was organised together with the CONCERT project SEPARATE. The main aim of this meeting was to present recent scientific data related to the impact of ionizing radiation on EV biology and function. A further specific aim was to present the latest findings generated in the two CONCERT projects. Additionally, some international experts on this area were invited to give a presentation. The meeting was a great success with more than 200 participants.

Final conclusions

The major scientific results generated by the project can be summarized as follows:

- We showed that ionizing radiation effects can be mediated by EVs in the haematopoietic system.
- We demonstrated that bone marrow changes caused by EVs originating from low dose irradiated mice were often similar albeit milder or less consistent to alterations induced by EVs from high dose irradiated mice.
- Although the direct role of EVs in modifying leukaemia incidence awaits further confirmation based on definitive data, it is clear that it has a role in inducing bone marrow abnormalities.
- The expression of certain miRNAs in bone marrow-derived EVs are dose dependent.
- blood-derived EVs are suitable candidates to identify leukaemia-related and radiation-related biomarkers
- The project elucidated the importance of the EV isolation method for different biological endpoints.
- An international training course was organised on radiation leukemogenesis.
- The major topics of the project as well as recent advances in radiation-related EV research were presented at a satellite meeting during the ICRR 2019, Manchester, UK, 25-29 August 20

Altogether, we succeeded to address the proposed objectives, namely 1) project results contributed to advance knowledge in leukaemogenesis in general and low dose radiation-induced leukaemogenesis in particular; 2) the project generated new data on radiation-associated signals transmitted by EVs and clarified novel aspects of low dose IR-induced bystander signalling mechanisms; 3) methodologically, we standardized EV isolation from BM and identified the specific limitations of different EV isolation techniques for certain endpoints, improved in vivo EV labelling and uptake, demonstrated for the first time that NANOSTRING is suitable for the study of EV miRNA content, also highlighting the limitations of the method, and optimized the FISH technique in interphase cells.